

Interactive comment on “**Microbial dormancy and its impacts on Arctic terrestrial ecosystem carbon budget**” by **Junrong Zha and Qianlai Zhuang**

Jens-Arne Subke (Editor)

jens-arne.subke@stir.ac.uk

Received and published: 24 January 2020

Dear Drs Zha and Zhuang,

Thank you for responding to the referee reports. Work on the manuscript has addressed many of the concerns by referees, and I am content with these (e.g. the issue of equifinality). However, I am not convinced that you have managed to alleviate the main point of referee 1, which is that the uncertainty associated with both models compared here is so large that it is not possible to judge any potential improvement from incorporating dormancy. I would therefore like to ask you to revise the manuscript further to address the issue of modelling uncertainty. I include some further specific explanations below.

***Response:** We highly appreciate Dr. Subke’s constructive comments. Below we detail how we have revised the manuscript by specifically further addressing the model uncertainty. We have also addressed some other minor comments regarding figure quality.*

I agree with referee 1 that model uncertainty is key for this comparison, and this is not well illustrated also in the revised paper. Figures 2, 4 and 5 show that in some instances the new model follows temporal dynamics better, but the improvement over the nondormancy model is not that clear, and in absence of explicit uncertainty associated with either model, the reader can not judge whether this is a significant improvement. This then leads to similar problems when making regional predictions – Are stated differences for the contrasting models within the model uncertainty?

***Response:** We used Fig. 2 to show dormancy model performance in comparison with observational data. We used different sets of observational data to verify both dormancy and nodormancy models in Figs. 4 and 5. While we acknowledge both models have various temporal dynamics in comparison with observational data, especially considering relatively large uncertainty associated with dormancy model (also for nodormancy model). However, we do see in general the dormancy model performs better. To confirm this, we plotted the linear model comparison with observational data for both models shown in Fig. 6. The comparison shows that the dormancy model MIC-TEM-Dormancy performs better with smaller intercepts and larger slopes that are closer to 1. For the simulated NEP of both models, we compared them with observational data in Table 5. In general, the dormancy model has relatively smaller intercepts while slopes and R values varying for various ecosystems. With recognition of these site-level uncertainties, we conducted ensemble simulations in the last revision to quantify the regional uncertainties for both models. Our results were presented with uncertainties in Figs. 11 and 12. Consequently, our conclusions were drawn by considering these uncertainties. In this revision, we revised the Abstract and Conclusion sections to reflect these changes concerning model differences and uncertain parameters and simulations by adding standard deviations.*

You also don't address fully the point that the dormancy model increases modelling uncertainty owing to the larger number of parameters. As no modelling uncertainty is quantified at present, I think that this fundamental limitation of constructing a more complex model (i.e. with more parameters) is not reflected appropriately. Figure 11 seems to show the wide band of uncertainty (but this is not clearly explained in the figure caption). Can the apparent difference/improvement of the model prediction be justified, given the considerable underlying uncertainty?

Response: *Thanks for the comments. We agree that adding the dormancy effects makes the model more complex by increasing number of parameters, which might increase model uncertainty. This is a fundamental modeling dilemma, i.e., shall we use a simpler model (less processes considered) or a more adequate model (more essential processes considered). In this study, we believe, the dormancy dynamics are an important process to be considered to more adequately capture microbial decomposition. Two versions of the model simulations and observational data comparisons for dominant ecosystems in the region indicate that the dormancy model better captures the observation while there are uncertainties for both models. We agree this study has not fully addressed this problem – which is subject to a research community debate. Therefore, in this revision, we added a paragraph to discuss this modeling dilemma, quoted below “While our analysis suggests it is important to incorporate microbial dormancy dynamics into a process-based biogeochemistry model to more adequately simulate carbon dynamics in northern high latitudes, we do confront modeling dilemmas. First, our process-based models have a relatively large number of parameters, which unavoidably creates the “equifinality” problem as recognized in our previous studies for the model (e.g., Tang and Zhuang, 2008, 2009). To alleviate this problem in this analysis, we have conducted parameter ensemble simulations at both site and regional levels and presented our results with uncertainties, which could be a standard approach for process-based complex biogeochemistry modeling analyses. Second, incorporating more ecosystem processes increases the number of parameters in our model, inducing even larger uncertainties for both site level and regional simulations. On the one hand, the more complex model to a certain degree helps capture observations, on the other hand, the model uncertainty has not been constrained or even enlarged. We highlight the need to further investigate this trade-off within the modeling research community.”.*

Some of the figures are still very hard to read. Axis labels and numbers are generally too small. Fig. 3, for example, is improved as far as resolution is concerned, but font size is far too small. The same applies to other figures.

Response: *Thanks much for the suggestion. In this revision, we improved the quality of these figures.*

Best regards, Jens-Arne Subke

1 **Microbial dormancy and its impacts on Arctic terrestrial ecosystem carbon budget**

2

3 Junrong Zha and Qianlai Zhuang

4

5 Department of Earth, Atmospheric, and Planetary Sciences and Department of Agronomy,
6 Purdue University, West Lafayette, IN 47907 USA

7

8 Submitted to: *Biogeoscience*

9

10 Correspondence to: qzhuang@purdue.edu

11

12

13

14

15

16

17

18

19

20

21

22

23

24

25

26

27

28

29

30

31

32

33

34

35

36

37

38

39

40

41

42

43

44

45

46

47 **Abstract**

48 **A large amount of soil carbon in the Arctic terrestrial ecosystems could be emitted as**
49 **greenhouse gases in a warming future. However, lacking detailed microbial processes such**
50 **as microbial dormancy in current biogeochemistry models might have biased the**
51 **quantification of the regional carbon dynamics. Here the effect of microbial dormancy was**
52 **incorporated into a biogeochemistry model to improve the quantification for the last and**
53 **this century. Compared with the previous model without considering the microbial**
54 **dormancy, the new model estimated the regional soils stored 75.9 Pg more C in the**
55 **terrestrial ecosystems during the last century, and will store 50.4 Pg and 125.2 Pg more C**
56 **under the RCP 8.5 and RCP 2.6 scenarios, respectively, in this century. This study**
57 **highlights the importance of the representation of microbial dormancy in earth system**
58 **models to adequately quantify the carbon dynamics in the Arctic.**

59

60

61

62

63

64

65

66

67

68

69

70

71

72

73

74

75

76 **1. Introduction**

77 The land ecosystems in northern high latitudes (>45 °N) occupy 22% of the global
78 surface and store over 40% of the global soil organic carbon (SOC) (McGuire & Hobbie, 1997;
79 Melillo et al., 1993; Tarnocai et al., 2009; Hugelius et al., 2014). During the past decades, a
80 greening accompanying a warming in the region has been documented (Zhou et al., 2001; Lloyd
81 et al., 2002; Stow et al., 2004; Callaghan et al., 2005; Tape et al., 2006). The regional carbon
82 dynamics are expected to loom large in the global carbon cycle and exert large feedbacks to the
83 global climate system (McGuire et al., 2009; Davidson & Janssens, 2006; Bond-Lamberty &
84 Thomson, 2010).

85 To date, numerous ecosystem models have been developed to project the feedbacks
86 between terrestrial ecosystem carbon cycling and climate (Raich et al., 1991; Zhuang et al.,
87 2001, 2002, 2015; Parton et al., 1993; Knorr et al., 2005; Running & Coughlan, 1988), but they
88 can bias their quantifications due to missing detailed microbial mechanisms in these models
89 (Schmidt et al., 2011; Todd-Brown et al., 2013; Conant et al., 2011; Treseder et al., 2011).
90 Microorganisms play a central role in decomposition of litter and soil organic carbon, which
91 further governs the global carbon cycling and climate change (Xu et al., 2014; Treseder et al.,
92 2011; Wang et al., 2015). An emerging field of research has begun to incorporate microbial
93 ecology into existing process-based models to represent decomposition in ways that include
94 important microbial processes that were previously ignored (Zha & Zhuang, 2018; Schimel &
95 Weintraub, 2003; Allison et al., 2010; German et al., 2012). These microbial-based models tend
96 to better reproduce field and satellite observations than traditional ones that treat soil
97 decomposition as a first-order decay process without considering microbial activities (Treseder
98 et al., 2011; Wieder et al., 2013; Todd-Brown et al., 2011; Lawrence et al., 2009; Moorhead et

99 al., 2006). However, some vital microbial traits such as microbial dormancy and community
100 shifts are still rarely explicitly considered in large-scale ecosystem models (Wieder et al., 2015),
101 and this may introduce notable uncertainties (Graham et al., 2014, 2016; Wang et al., 2015;
102 Bouskill et al., 2012; Kaiser et al., 2014).

103 Dormancy is broadly recognized as a strategy for microorganisms to cope with periodical
104 environmental stresses (Harder & Dijkhuizen, 1983). When environmental conditions are
105 unfavorable for growth, microbes switch to a dormant state, which is a reversible state of low to
106 zero metabolic activity (Stolpovsky et al., 2011; Lennon & Jones, 2011). In this state,
107 biogeochemical processes such as soil decomposition are slow (Blagodatskaya et al., 2013). At
108 any given time, there is only a fraction of, likely below 50%, metabolically active microbes in
109 natural soils (Wang et al., 2015; Stolpovsky et al., 2011). Soil decomposition and nutrient
110 cycling mainly depend on these active microbes because only active ones can consume organic
111 matter and replicate themselves (Wang et al., 2015; Blagodatskaya et al., 2014). To date, most
112 existing biogeochemistry models use total rather than active microbial biomass as an indicator of
113 microbial activities (Wieder et al., 2015), which could bias the estimates of soil decomposition
114 and ecosystem carbon budget (Hagerty et al., 2014; He et al., 2015). Especially, the Arctic
115 terrestrial ecosystems are nitrogen-limited, neglecting microbial dormancy will lead to incorrect
116 estimates of nitrogen availability through soil decomposition, failing to capture nitrogen
117 feedbacks to carbon dynamics (Wang et al., 2015; Stolpovsky et al., 2011; Thullner et al., 2005).
118 Furthermore, the Arctic has experienced a marked seasonality of active and dormant microbial
119 cycles and the above-global-average warming, which might have increased the proportion of
120 active microbes in soils (He et al., 2015). Thus, incorporating dormancy effects will improve
121 model realism to provide a better projection of the Arctic carbon dynamics.

122 This study incorporated the effects of microbial dormancy trait into an extant process-
123 based biogeochemistry model (MIC-TEM) (Zha & Zhuang, 2018; He et al., 2015). The dormant
124 and active microbial physiology has been considered explicitly in the new version of model
125 (MIC-TEM-dormancy). The revised model was parameterized, validated, and then applied to
126 evaluate the carbon dynamics during the last and this centuries in the Arctic terrestrial
127 ecosystems (north 45 °N above). By comparing the results of MIC-TEM-dormancy and MIC-
128 TEM, we can show that incorporating microbial dormancy may produce a much different
129 prediction in historical and future carbon budget.

130

131 **2. Methods**

132 **2.1 Overview**

133 Due to the importance of microbial dormancy, some recent work has been done to consider
134 the metabolic activation and deactivation of microbes in soil and its effects on soil carbon (C)
135 dynamics and climate feedbacks. For example, Wang et al. (2015) has incorporated transformation
136 processes between active and dormant states to develop two versions of MEND, that is, MEND
137 with and without dormancy. The two versions of the model have been applied to quantify the
138 carbon decomposition in laboratory incubations of four soils. Salazar et al. (2018) have also taken
139 microbial dormancy into account to compare their predictions of microbial biomass and soil
140 heterotrophic respiration (R_H) under simulated cycles of stressful (dryness) and favorable (wet
141 pulses) conditions. Our study extends those modeling studies to the whole Arctic region by
142 developing a more detailed biogeochemistry model considering the dormancy impacts. Below, we
143 first describe how we developed the new model (MIC-TEM-dormancy) by incorporating the
144 microbial dormancy trait into an existing microbial-based biogeochemistry model (MIC-TEM).

145 Second, we discuss how parameterization and validation of MIC-TEM-dormancy model were
146 conducted using observed net ecosystem exchange data, and heterotrophic respiration data at
147 representative sites. Third, we presented how the model was applied to northern high latitudes
148 (above 45 °N) for the 20th and 21st centuries and discussed the dormancy effects on regional carbon
149 budget.

150

151 **2.2 Model description.**

152 A non-dormancy version of biogeochemistry model (MIC-TEM) has been developed by
153 incorporating a microbial module (Allison et al., 2010) into an extant large-scale biogeochemical
154 model (TEM) to explicitly (Zhuang et al., 2003) consider the effects of microbial dynamics and
155 enzyme kinetics on carbon dynamics (Zha & Zhuang, 2018). Here we further advanced the MIC-
156 TEM by incorporating algorithms that describe the effects of microbial dormancy dynamics
157 based on He et al. (2015). Different from He et al. (2015), in which microbial module was driven
158 with existing data of carbon stocks and fluxes, our study incorporated the microbial module into
159 an extant MIC-TEM that simulates carbon data dynamically. This coupling enables us to
160 extrapolate our model to whole northern high-latitudes region, rather than only for temperate
161 forest region in He et al. (2015). In our new model (MIC-TEM-dormancy), microbial biomass
162 pool was divided into two fractions, including the dormant and active microbial biomass pools.
163 The two microbial biomass pools and the reversible transition between them have been
164 considered explicitly in the new model (Figure 1), which was ignored in MIC-TEM.

165 In previous MIC-TEM, heterotrophic respiration (R_H) is calculated as:

$$166 \quad R_H = \text{ASSIM}_x \times (1 - \text{CUE}) \quad (1)$$

167 Where ASSIM and CUE represent microbial assimilation and carbon use efficiency, respectively.
 168 For detailed carbon dynamics in MIC-TEM, see Zha & Zhuang (2018).

169 Here we revised MIC-TEM by incorporating microbial dormancy dynamics according to
 170 He et al. (2015). In MIC-TEM-dormancy, the soil heterotrophic respiration R_H is comprised of
 171 three parts: the maintenance respiration from the active and dormant microorganisms and the CO_2
 172 production through the process of microbial assimilation (He et al., 2015):

$$173 \quad R_H = m_R Q_{10mic}^{\frac{temp-15}{10}} B_a + \beta m_R Q_{10mic}^{\frac{temp-15}{10}} B_d + CO_2 \quad (2)$$

174 where the first two terms are maintenance respiration from the active and dormant
 175 microorganisms, respectively. The last term is the CO_2 produced during the process of microbial
 176 assimilation.

177 For first two terms, B_a and B_d represents the active and dormant microbial biomass pool,
 178 respectively. The parameter m_R denotes the specific maintenance rate at active state (h^{-1}), and β
 179 is the ratio of dormant maintenance rate to active maintenance rate. Thus, βm_R denotes the
 180 maximum specific maintenance rate at dormant state. Temperature sensitivity was expressed as
 181 the Q_{10} function ($Q_{10}^{\frac{temp-15}{10}}$), where temp is soil temperature at top 20 cm (units: $^{\circ}C$).

182 For the third term, the CO_2 produced through microbial assimilation is calculated as in He et al.
 183 (2015) and Allison et al. (2010):

$$184 \quad CO_2 = ASSIM \times (1 - Y_g) \quad (3)$$

185 Where ASSIM represents the microbial assimilation and the parameter Y_g represents carbon use
 186 efficiency. Microbial assimilation (ASSIM) is calculated as in He et al. (2015):

$$187 \quad ASSIM = \frac{1}{Y_g} \frac{\Phi}{\alpha} m_R Q_{10enz}^{\frac{temp-15}{10}} B_a \left(\frac{CN_{soil}}{CN_{mic}} \right)^{0.6} \quad (4)$$

188 Here parameter α is maintenance weight (h^{-1}), CN_{soil} and CN_{mic} denotes the C:N ratios of soil and
 189 that of microbial biomass. Besides, Φ is the substrate saturation level and defined as in He et al.
 190 (2015) and Wang et al. (2014):

$$191 \quad \Phi = \frac{S}{K_s + S} \quad (5)$$

192 Where K_s is the half saturation constant for substrate uptake as indicated by the Michaelis–Menten
 193 kinetic, and S is soluble C substrates that are directly accessible for microbial assimilation (Wang
 194 et al., 2014). Here we quantified concentration of soluble C substrates that are directly accessible
 195 for microbial assimilation by using conceptual framework from Davidson et al. (2012):

$$196 \quad S = \text{Soluble C} \times \frac{D_{liq}}{\theta^3} \quad (6)$$

197 The term ‘Soluble C’ denotes the state variable of soluble carbon pool. D_{liq} is the diffusion
 198 coefficient of the substrate in the liquid phase, and is formulated as:

$$199 \quad D_{liq} = 1/(1-BD/PD)^3 \quad (7)$$

200 Where BD is the bulk density and PD is the soil particle density. θ is the volumetric soil moisture.
 201 Different from MIC-TEM, the transitions between active and dormant microbial biomass are
 202 included in MIC-TEM-dormancy.

$$203 \quad B_{a \rightarrow d} = (1 - \Phi) m_R Q_{10mic}^{\frac{temp-15}{10}} B_a \quad (8)$$

$$204 \quad B_{d \rightarrow a} = \Phi m_R Q_{10mic}^{\frac{temp-15}{10}} B_d \quad (9)$$

205 Where $B_{a \rightarrow d}$ and $B_{d \rightarrow a}$ denote the transition from the active to dormant microbe and from the
 206 dormant to active microbe, respectively (He et al., 2015; Wang et al., 2014). Thus, dormancy rate
 207 is affected by active and dormant biomass, soil temperature ($temp$) and soil moisture (θ in Φ).

208 The active microbial biomass (B_a) is modeled as (He et al., 2015; Wang et al., 2014):

$$209 \quad \frac{dB_a}{dt} = \text{ASSIM} \times Y_g - m_R Q_{10mic}^{\frac{temp-15}{10}} B_a - B_{a \rightarrow d} + B_{d \rightarrow a} - \text{DEATH} - \text{EPROD} \quad (10)$$

210 Where DEATH and EPROD denotes microbial biomass death and enzyme production, which are
 211 modeled as proportional to active microbial biomass with constant rates r_{death} and r_{EnzProd} (Allison
 212 et al., 2010):

$$213 \quad \text{DEATH} = r_{\text{death}} \times \text{Ba} \quad (11)$$

$$214 \quad \text{EPROD} = r_{\text{EnzProd}} \times \text{Ba} \quad (12)$$

215 Where r_{death} and r_{EnzProd} are the rate constants of microbial death and enzyme production,
 216 respectively.

217 The dormant microbial biomass (B_d) is modeled as (He et al., 2015; Wang et al., 2014):

$$218 \quad \frac{dB_d}{dt} = -\beta m_R Q_{10\text{mic}}^{\frac{\text{temp}-15}{10}} B_d + B_{a \rightarrow d} - B_{d \rightarrow a} \quad (13)$$

219 The Soluble C pool is modeled as (He et al., 2015; Allison et al., 2010):

$$220 \quad \frac{d \text{Soluble C}}{dt} = \text{DECAY} - \text{ASSIM} + \text{ELOSS} + \text{DEATH} \quad (14)$$

221 Where DECAY represents the enzymatic decay of soil organic carbon (SOC), and ELOSS
 222 represents the loss of enzyme.

223 DECAY is regulated by enzyme biomass (ENZ), soil organic carbon (SOC), soil temperature, and
 224 substrate quality (He et al., 2015):

$$225 \quad \text{DECAY} = V_{\text{max}} \times Q_{10\text{enz}}^{\frac{\text{temp}-15}{10}} \times \text{ENZ} \times \frac{\text{SOC}}{K_{m\text{uptake}} + \text{SOC}} \times (120 - \text{CN}_{\text{soil}}) \quad (15)$$

226 Where V_{max} is the maximum SOC decay rate, $K_{m\text{uptake}}$ is half saturation constant for enzymatic
 227 decay.

228 ELOSS is modeled as a first-order process (Allison et al., 2010) to represent enzyme turnover:

$$229 \quad \text{ELOSS} = r_{\text{enzloss}} \times \text{ENZ} \quad (16)$$

230 Where r_{enzloss} is the rate constant of enzyme loss.

231 The soil organic carbon pool (SOC) is modeled as:

232
$$\frac{dSOC}{dt} = \text{Litterfall} - \text{DECAY} \quad (17)$$

233 Where Litterfall is estimated as a function of vegetation carbon (Zhuang et al., 2010).

234 Last, enzyme pool (ENZ) is modeled as:

235
$$\frac{dENZ}{dt} = \text{EPROD} - \text{ELOSS} \quad (18)$$

236 With the modification of microbial carbon dynamics by considering microbial life-history trait,
237 soil decomposition is changed since it is controlled by microbes. When microbial dormancy is
238 considered, the number of active microbes that participate in soil decomposition is much less. The
239 changes in soil decomposition directly influence the amount of soil respiration, and further
240 influence soil nitrogen (N) mineralization that determines soil N availability for plants, affecting
241 gross primary production (GPP). Since both GPP and R_H can be affected by microbial dormancy,
242 net ecosystem production (NEP) will also be affected.

243

244 **2.3 Model parameterization and validation**

245 The detailed description of parameters that are related to microbial dormancy can be found
246 in He et al. (2015) (Table 1). Here we calibrated the MIC-TEM-dormancy at six representative
247 sites with gap-filled monthly net ecosystem productivity (NEP, $\text{gCm}^{-2}\text{mon}^{-1}$) data in northern high
248 latitudes (Table 2). Site-level climatic data and soil texture data were organized for driving model.
249 All sites information can be found on AmeriFlux network (Davidson et al., 2000). The results for
250 model parameterization were presented in Figure 2. We conducted the parameterization using a
251 global optimization algorithm known as SCE-UA (Shuffled complex evolution) method (Duan et
252 al., 1994). An ensemble of 50 independent sets of parameters were performed based on prior ranges
253 from literature (Table 1) to minimize the difference between the monthly simulated and measured
254 NEP at the chosen sites. The cost function of the minimization is:

255
$$\text{Obj} = \sum_{i=1}^k (\text{NEP}_{\text{obs},i} - \text{NEP}_{\text{sim},i})^2 \quad (17)$$

256 Where $\text{NEP}_{\text{obs},i}$ and $\text{NEP}_{\text{sim},i}$ are the observed and simulated NEP, respectively. k is the number of
257 data pairs for comparison. Except for the parameters of microbial dormancy, other parameters are
258 derived directly from MIC-TEM (Zha & Zhuang, 2018). The optimized parameters were used for
259 model validation and regional simulations.

260 For model validation, we chose another six sites that containing monthly NEP data from
261 AmeriFlux network (Table 3). Moreover, we also conducted site-level validations with monthly
262 soil respiration data from AmeriFlux network and Fluxnet dataset. The site information was
263 provided in Table 4. For these sites, we assumed 50% of soil respiration was heterotrophic
264 respiration (R_H) for forest (Hanson et al., 2000), 60% and 70% of that was R_H for grassland (Wang
265 et al., 2009) and tundra (Billings et al., 1977). Because there is a limited amount of available R_H
266 data, we could not conduct a regional validation for all pixels in northern high latitudes. Instead,
267 we extracted 61 sites providing data of average annual heterotrophic respiration from ORNL global
268 Soil Respiration Dataset (https://daac.ornl.gov/SOILS/guides/SRDB_V4.html, Bond-Lamberty et
269 al., 2018) for model validation. The site-level observed average annual R_H was used to compare
270 with simulated annual R_H by MIC-TEM-dormancy and MIC-TEM. The MIC-TEM-dormancy was
271 run at monthly time step to keep consistent with the time step of MIC-TEM. Although microbial
272 dynamics occur at fine temporal scales (Tang & Riley, 2014), we can still quantify the cumulative
273 impacts of microbial dynamics on carbon and nitrogen cycling at monthly time by not changing
274 the model structure.

275

276 **2.4 Spatial extrapolation**

277 For historical simulations during the 20th century, two sets of regional simulations using
278 MIC-TEM-dormancy and MIC-TEM at a spatial resolution of 0.5° latitude × 0.5° longitude were
279 conducted. Our model simulation contains two parts: spin-up and transient simulation. A typical
280 spin-up was conducted to get the model to a steady state for each spatial location, which will be
281 used as initial conditions for transient simulations (McGuire et al., 1992). During spin-up
282 procedure, cyclic forcing data was used to force the model run, and repeated continuously until
283 dynamic equilibrium was achieved at which the modeled state variables show a cyclic pattern or
284 become constant. Specifically, this study used the monthly historical climate data from 1900 to
285 1940 to repeatedly drive the model for the spin-up. Before spin-up procedure, the model was
286 initialized with default built-in carbon stocks (Raich et al., 1991). During transient simulations,
287 the calibrated ecosystem-specific parameters were used for regional simulations. The previous
288 dynamic equilibrium was used as initial value for transient simulation. The historical climatic
289 forcing data, including the monthly air temperature, precipitation, cloudiness, and atmospheric
290 CO₂ concentrations, were organized from the Climatic Research Unit (CRU TS3.1) from the
291 University of East Anglia (Harris et al., 2014). We also used gridded data of soil texture (Zhuang
292 et al., 2003), elevation (Zhuang et al., 2015), and potential natural vegetation (Melillo et al., 1993)
293 from literatures. In our model, we assumed that soil texture, elevation, and potential natural
294 vegetation data only vary spatially, not vary over time (Zhuang et al., 2015).

295 In addition, regional simulations over the 21st century were conducted under two
296 Intergovernmental Panel on Climate Change (IPCC) climate scenarios (RCP 2.6 and RCP 8.5).
297 The future climatic forcing data under these two climate change scenarios were derived from the
298 HadGEM2-ESmodel, which is a member of CMIP5project213 ([https://esgf-](https://esgf-node.llnl.gov/search/cmip5/)
299 [node.llnl.gov/search/cmip5/](https://esgf-node.llnl.gov/search/cmip5/)). Then the regional estimations were obtained by summing up the

300 gridded outputs for our study region. The positive simulated NEP represents a CO₂ sink from the
301 atmosphere to terrestrial ecosystems, while a negative value represents a source of CO₂ from
302 terrestrial ecosystems to the atmosphere.

303 **2.5 Parameter equifinality effects**

304 Our previous studies using TEM has demonstrated that equifinality derived from site-level
305 parameterization will affect the uncertainty in the estimation of regional carbon dynamics (Tang
306 and Zhuang, 2008, 2009). Here equifinality refers to that a number of sets of parameters result in
307 model simulations that all match the data similarly well. To quantify this effect on our simulation
308 uncertainty, we conducted ensemble regional simulations with 50 sets of parameters for both
309 historical and future studies. The 50 sets of parameters were obtained according to the method in
310 Tang and Zhuang (2008).

311 **3. Results**

312 **3.1 Inversed Model Parameters and model validation**

313 Using SCE-UA ensemble method, 50 independent sets of parameters were converged to
314 minimize the objective function. Then the optimized parameters are calculated as the mean of these
315 50 sets of inversed parameters. The boxplot of parameter posterior distributions reflects different
316 ecosystem properties at these sites (Figure 3). For instance, growth yield was higher in tundra types
317 than in forests, meaning microorganisms in environment with higher energy limitation tend to
318 enhance the efficiency of energy transportation. Besides, alpha, the maintenance weight, was also
319 higher in tundra types than in forests. From the plot for parameter beta, the ratio of dormant
320 maintenance rate to specific maintenance rate for active biomass in tundra types is lower than that
321 in forest types. Other microbial related parameters did not differentiate much among different
322 vegetation types.

323 After parameterization, the MIC-TEM-dormancy was validated with monthly NEP data for
324 six representative ecosystems, and the comparisons between monthly observed NEP and
325 simulated NEP were presented in Figure 4. With the optimized parameters, the dormancy-based
326 model was used to reproduce NEP to compare with the measured NEP (Table 5). The R^2 ranges
327 from 0.67 for Atqasuk to 0.93 for Bartlett Experimental Forest (Table 5). Generally, our new
328 model performs better for forest ecosystems than for tundra ecosystems. Compared with MIC-
329 TEM, dormancy model performs better for alpine tundra, temperate coniferous forest, and
330 grassland. For other sites, both models show similar performance (Table 5). Besides, a set of
331 monthly soil respiration data were selected to evaluate the estimated R_H . The comparisons
332 between monthly observed R_H and simulated R_H from two contrasting models were conducted
333 (Figure 5). MIC-TEM-dormancy has higher R^2 and lower root mean square error (RMSE) (Table
334 6). Sixty-one sites with average annual R_H in northern high-latitude regions were used to further
335 evaluate the new model performance. The dormancy model has lower intercept and slope with R^2
336 of 0.45, while R^2 of MIC-TEM is 0.3 (Figure 6). These analyses indicate that new model is more
337 realistic in representing R_H by considering microbial dormancy. This difference in R_H further
338 affects soil available nitrogen dynamics, influencing nitrogen uptake by plants, the rate of
339 photosynthesis and NPP (Zhuang et al., 2015; Zha et al., 2018; Thullner et al., 2005).

340

341 **3.2 Regional carbon dynamics during the 20th century**

342 Regional extrapolation with both models estimated a regional carbon sink but with different
343 magnitudes (Figure 7c). With optimized parameters, MIC-TEM estimated a regional carbon sink
344 of 77.6 Pg with the interannual standard deviation of 0.21 Pg C yr⁻¹ during the 20th century.
345 However, MIC-TEM-dormancy nearly doubles the sink at 153.5 Pg with the interannual standard

346 deviation of $0.12 \text{ Pg C yr}^{-1}$ during the last century (Figure 7c). At the end of the century, MIC-
347 TEM estimated that NEP reaches 1.0 Pg C yr^{-1} in comparison with MIC-TEM-dormancy estimates
348 of 1.5 Pg C yr^{-1} (Figure 7c). Both models simulated similar trends for regional NPP, R_H and NEP
349 (Figure 7). Generally, they show an increasing trend in the 20th century (Figure 7). Meanwhile,
350 with optimized parameters, MIC-TEM-dormancy estimated NPP and R_H at $7.94 \text{ Pg C yr}^{-1}$ and 6.4
351 Pg C yr^{-1} , which are 5.8% and 16.3% less than the estimations from MIC-TEM, respectively
352 (Figures 7a and 7b). This pronounced difference of NEP between two models comes from the
353 disparity between the simulated NPP and R_H with them since NEP is calculated as the difference
354 between NPP and R_H . Without considering dormancy, MIC-TEM estimates more active microbial
355 biomass since it assumes the whole microbial biomass pool will participate in soil decomposition.
356 The fact is only active part of microbial biomass can affect organic matter decomposition, meaning
357 MIC-TEM overestimates R_H . On the other hand, overestimation of R_H can induce higher nitrogen
358 uptake by plants, which will accelerate rate of photosynthesis and further enhance NPP projection.
359 Although MIC-TEM estimates higher NPP and R_H than MIC-TEM-dormancy does, NEP estimated
360 from MIC-TEM is actually lower.

361 The average annual seasonal patterns of NPP, R_H and NEP during the 1990s were also
362 organized from regional simulations with two models (Figure 8). Temporally, both models
363 projected higher NPP and R_H in summer than in winter (Figures 8a and 8b) due to higher soil
364 temperature and moisture (McGuire et al., 1992). Setting the R_H projection from MIC-TEM as a
365 baseline, MIC-TEM-dormancy averagely projected 33% less R_H in summer (May to September),
366 and 30% more in winter (other months) (Figure 8b), which indicates that without dormancy,
367 model tends to estimate lower soil respiration compared to dormancy model due to ignorance of
368 dormant respiration in winter but estimate higher soil respiration due to higher estimation of

369 active biomass in summer. In the meantime, seasonal cycle of NPP with MIC-TEM-dormancy
370 shows a relative flattening pattern compared with MIC-TEM, which is similar to seasonal cycle
371 of R_H (Figure 8a). Though R_H and NPP show the similar seasonal patterns, NEP can still show
372 different pattern. Here seasonal cycles of NEP with models are close to each other (Figure 8c),
373 but dormancy model projected slightly higher NEP in summer.

374 **3.3 Regional carbon dynamics during the 21st century**

375 Under the RCP 8.5 scenario, both models estimated the region acts as a carbon sink (Figure
376 9). The MIC-TEM-dormancy predicted a C accumulation of 129.9 Pg by the end of this century.
377 with the interannual standard deviation of 0.13 Pg C yr⁻¹, whereas MIC-TEM estimates a C
378 accumulation of 79.5 Pg -with the interannual standard deviation of 0.37 Pg C yr⁻¹ during the 21st
379 century (Figure 9). Thus, MIC-TEM-dormancy estimates an increase of 50.4 Pg regional carbon
380 sequestration relative to MIC-TEM, with less interannual variation (Figure 9). Under this
381 scenario, both models predict similar temporal trends for NEP, namely increasing from the 2000s
382 and then decreasing from the 2070s onward (Figure 9). MIC-TEM-dormancy predicts that
383 carbon sink reaches 1.36 Pg C yr⁻¹ in the 2090s, which is 0.26 Pg C yr⁻¹ more than projection of
384 MIC-TEM. Moreover, MIC-TEM-dormancy estimated NPP and R_H at 10.2 Pg C yr⁻¹ and 8.9 Pg
385 C yr⁻¹, which are 1.3 Pg C yr⁻¹ and 1.8 Pg C yr⁻¹ less than the estimations from MIC-TEM,
386 respectively (Figure 9).

387 Under the RCP 2.6 scenario, the cumulative NEP from two models diverged by 125.2 Pg C
388 by 2100. The trajectory of inter-annual NEP estimated with the two models also diverged. The
389 MIC-TEM predicted the region fluctuates between carbon sinks and sources, and totally acts as a
390 carbon source of 1.6 Pg C with the interannual standard deviation of 0.24 Pg C yr⁻¹ during the
391 21st century. In contrast, MIC-TEM-dormancy projected the region acts as a carbon sink of 123.6

392 Pg C with an interannual standard deviation of 0.1 Pg C yr⁻¹ (Figure 9). MIC-TEM-dormancy
393 estimates NPP and R_H at 9.9 Pg C yr⁻¹ and 8.7 Pg C yr⁻¹, which are 0.5 Pg C yr⁻¹ and 1.7 Pg C yr⁻¹
394 ¹ less than the estimations from MIC-TEM, respectively (Figure 9). Moreover, simulations under
395 the two contrasting climate scenarios (RCP 2.6 and RCP 8.5) exhibit a large difference of 81.1
396 Pg C of cumulative NEP during the 21st century by MIC-TEM, but only 6.3 Pg C of that by
397 MIC-TEM-dormancy. This difference indicates microbes provide a resistant response to climate
398 change due to dormancy to some extent (Treseder et al., 2011).

399 The average annual seasonal patterns of NPP, R_H and NEP during the 2990s by two
400 models were also presented (Figure 10). MIC-TEM-dormancy estimated higher R_H in winter, but
401 lower R_H in summer under both future scenarios (Figure 10). NPP is the same in winter with or
402 without dormancy, and in the late summer is higher than that without dormancy, especially in the
403 RCP 8.5 scenario. The combined flattening patterns of NPP and R_H result in different patterns
404 for NEP. Under the RCP 2.6 scenario, MIC-TEM-dormancy predicts higher NEP from June to
405 October, but lower NEP from January to April compared to MIC-TEM (Figure 10). Under the
406 RCP 8.5 scenario, MIC-TEM-dormancy predicts higher NEP from June to September, but much
407 lower NEP in other months than MIC-TEM (Figure 10).

408 **3.4 Regional uncertainty considering equifinality effects during 20th and 21st centuries**

409 The ensemble simulations for the 20th century is shown in Figure 11. Given the
410 uncertainty in parameters, MIC-TEM-dormancy predicted that the regional cumulative carbon
411 ranges from a carbon loss of 28.2 Pg to a carbon sink of 362.1 Pg by different ensemble
412 members, with a mean of 71.2±54.8 Pg (Figure 11). For the 21st century, MIC-TEM-dormancy
413 predicted that the region acts from a carbon source of 49.3 Pg C to a carbon sink of 296.5 Pg C,
414 with a mean of 112.7±116.5 Pg under the RCP 2.6 scenario (Figure 12). Under the RCP 8.5

415 scenario, MIC-TEM-dormancy predicted that the region acts from a carbon source of 27.1 Pg C
416 to a carbon sink of 401.3 Pg C, with a mean of 143.1 ± 162.5 Pg (Figure 12).

417 **4. Discussion**

418 Soils are the largest carbon repository in the terrestrial biosphere and hold 2.5 times more
419 carbon than the atmosphere (Frey et al., 2013; Schlesinger & Andrews, 2000). Especially, a
420 significant portion of soil organic carbon stored in northern high latitudes (Tarnocai et al., 2009).
421 Besides, the magnitude of the warming in these regions is larger, almost twice, that of the global
422 average (Serreze & Francis, 2006) and the changing climate is expected to alter the carbon cycle
423 through influencing the activities of microorganisms in controlling soil decomposition (Manzoni
424 et al., 2012; Melillo et al., 2011). Therefore, explicit consideration of microbial traits and
425 functions in large-scale biogeochemistry models is necessary for better quantification of carbon-
426 climate feedbacks (Thullner et al., 2005; Wang et al., 2015). Our regional simulations with two
427 contrasting models (MIC-TEM, MIC-TEM-dormancy) indicate the region was a carbon sink in
428 past decades, which is consistent with results from other process-based models (White et al.,
429 2000; Houghton et al., 2007; McGuire et al., 2009; Schimel, 2013). However, the magnitudes of
430 this sink are quite different in two models. Moreover, MIC-TEM-dormancy predicts the sink will
431 decrease under both RCP 8.5 and RCP 2.6 scenarios during the 21st century, while MIC-TEM
432 projects that the sink will increase under the RCP 8.5 but change to carbon source under the RCP
433 2.6 scenario. Estimations based on models without dormancy could fit observations of R_H as well
434 as estimations with dormancy, but at the cost of underestimating microbial biomass (Wang et al.,
435 2014). Differences in predicted R_H with and without dormancy increase with temperature and
436 with the length of the dry periods between wetting events (Salazar et al., 2018). The large
437 difference in two models suggests the importance of incorporating microbial dormancy effects.

438 The large bias between dormancy and non-dormancy models mainly comes from two parts.
439 First, many important microbial activities such as soil organic carbon decomposition and nutrient
440 cycling largely depend on the active fraction of microbial communities, not total microbial
441 biomass (Wang et al., 2014; Blagodatsky et al., 2000). However, only a small part (about 0.1-
442 2%, seldom exceed 5%) of the total soil microbial biomass is recognized to be active under
443 natural conditions (Blagodatsky et al., 2011; Werf & Verstraete, 1987). Thus, dormancy could be
444 a prominent feature in soil systems (Wang et al., 2014). Without considering dormancy, the
445 “effective” microbial biomass for soil decomposition could be overestimated, resulting in
446 overestimation of heterotrophic respiration (He et al., 2015). He et al. (2015) predicted total soil
447 R_H of all temperate forests (25°N-50°N) from the dormancy model amounted to 7.28 Pg C yr⁻¹
448 and 8.83 Pg C yr⁻¹ from a no-dormancy model, which is 21.3% higher than the dormancy model.
449 Although their study region and simulation period are different from our study, the results can
450 still be comparable. Both studies indicated that the magnitude of R_H from no-dormancy model
451 are higher than dormancy models. Second, high soil respiration stimulates N mineralization in
452 soils (Zhuang et al., 2001, 2002), making more nutrients for photosynthesis of plants (Raich et
453 al., 1991; McGuire et al., 1995). Therefore, NPP will be higher due to the N enrichment from
454 higher R_H . However, how NEP will change is still unclear. Our estimates of the northern
455 extratropical NEP in the 1980s (1.61 Pg C yr⁻¹ with MIC-TEM-dormancy and 0.84 Pg C yr⁻¹
456 with MIC-TEM) are within ranges (0.6 to 2.3 PgC yr⁻¹) reported in the literature for northern
457 regions (Schimel et al., 2001). Moreover, our predicted time trajectory of NEP in the 21st
458 century under the RCP 2.6 scenario is very similar to the finding of White et al. (2000),
459 indicating that NEP increases from the 2000s to the 2070s, and then decreases in the 2090s.
460 Although our dormancy model can project reasonable carbon fluxes and indicate the importance

461 of incorporating microbial dormancy when compared with MIC-TEM (Zha & Zhuang et al.,
462 2018), there are some other microbial traits have not yet been considered in our model. For
463 instance, one vital common evolutionary trait of microbe is the community shift (Wang et al.,
464 2015) with changing environment, including warming, N fertilization and precipitation (Treseder
465 et al., 2011; Frey et al., 2013; Allison et al., 2009; Evans & Wallenstein, 2011). Community shift
466 will influence microbial physiology, temperature sensitivity and growth rates (Classen et al.,
467 2015), which will further affect the rate of soil decomposition and other carbon dynamics
468 (Treseder et al., 2011; Schimel & Schaeffer, 2012; Todd-Brown et al., 2011). Besides, microbial
469 community composition was ignored in our model. We didn't separate among functional
470 microbial groups, but gather microbes into one "box". However, microbial community
471 composition could influence ecosystem functioning, and their variance in responses to
472 environmental conditions could alter the prediction of the rates of decomposition of organic
473 material (Balser et al. 2002; Fierer et al. 2007). Especially, some narrowly-distributed functions
474 can be more sensitive to microbial community composition, and these might benefit most from
475 explicit consideration of distinguishing functional groups in ecosystem models (McGuire &
476 Treseder, 2010; Schimel 1995). Thus, functional dissimilarity in microbial communities can be
477 considered in next step for model development (Strickland et al., 2009; Moorhead et al., 2006).
478 Moreover, microbial acclimation, a mechanism of adaption to a new temperature regime, is
479 another important trait to affect soil decomposition. Recent studies have found that the warming-
480 induced elevated respiration of the microbial community could decrease over time because of
481 acclimation (Melillo et al. 1993; Todd-Brown et al., 2011). This mechanism shall be factored
482 into future soil decomposition analysis.

483 Except for model limitations mentioned above, additional uncertainties may come from
484 inadequate model parameterization and model assumptions. For example, a critical microbial
485 parameter, carbon use efficiency (CUE), is a primary control to soil CO₂ efflux. Higher CUE
486 indicates more microbial growth and more carbon uptake by plants, while lower CUE indicates
487 higher soil decomposition (Manzoni et al., 2012). Theoretical and empirical studies have
488 suggested that CUE depends on both temperature and substrate quality (Frey et al., 2013) and
489 decreases as temperature increases and nutrient availability decreases (Manzoni et al., 2012).
490 Our study considered the CUE sensitivity to temperature, but not nutrient availability. On the
491 other hand, some model assumptions can also cause uncertainties. For example, we assumed that
492 vegetation will not change during the transient simulation. However, over the past few decades
493 in northern high latitudes, temperature increases have led to vegetation shift from one type to
494 another (Hansen et al., 2006; White et al., 2000). The vegetation changes will affect carbon
495 cycling in these ecosystems.

496 While our analysis suggests it is important to incorporate microbial dormancy dynamics
497 into a process-based biogeochemistry model to more adequately simulate carbon dynamics in
498 northern high latitudes, we do confront modeling dilemmas. First, our process-based models
499 have a relatively large number of parameters, which unavoidably creates the “equifinality”
500 problem as recognized in our previous studies for the model (e.g., Tang and Zhuang, 2008,
501 2009). To alleviate this problem in this analysis, we have conducted parameter ensemble
502 simulations at both site and regional levels and presented our results with uncertainties, which
503 could be a standard approach for process-based complex biogeochemistry modeling analyses.
504 Second, incorporating more ecosystem processes increases the number of parameters in our
505 model, inducing even larger uncertainties for both site level and regional simulations. On the

506 [one hand, the more complex model to a certain degree helps capture observations, on the other](#)
507 [hand, the model uncertainty has not been constrained or even enlarged. We highlight the need to](#)
508 [further investigate this trade-off within the modeling research community.](#)

512 **5. Conclusions**

513 This study incorporated microbial dormancy into a detailed microbial-based soil
514 decomposition biogeochemistry model to examine the fate of large Arctic soil carbon under
515 changing climate conditions. Regional simulations using MIC-TEM-dormancy indicated that,
516 over the 20th century, the region is a carbon sink of ~~166.8 ± 97.7~~ ~~153.5~~ Pg. This sink could
517 decrease to ~~175.9 ± 105.4~~ ~~129.9~~ Pg under the RCP 8.5 scenario or ~~125.4 ± 85.5~~ ~~123.6~~ Pg under
518 the RCP 2.6 scenario during the 21st century. Whether considering microbial dormancy or not
519 can cause large differences in soil decomposition estimation between two models. Meanwhile,
520 due to available nitrogen affected by soil decomposition, net primary production is consequently
521 influenced in these two centuries. The combined changes in soil decomposition and net primary
522 production led to large differences in carbon budget estimation between two models. Compared
523 with MIC-TEM, MIC-TEM-dormancy projected 75.9 Pg more C stored in the terrestrial
524 ecosystems over the last century, 50.4 Pg and 125.2 Pg more C under the RCP 8.5 and RCP 2.6
525 scenarios, respectively. This study highlights the importance of the representation of microbial
526 dormancy in earth system models in order to adequately quantify the carbon dynamics in
527 northern high latitudes.

528

529 **Acknowledgments**

530 This research was supported by a NSF project (IIS-1027955), a DOE project (DE-SC0008092),
531 and a NASA LCLUC project (NNX09AI26G) to Q. Z. We acknowledge the Rosen High
532 Performance Computing Center at Purdue for computing support. We thank the National Snow
533 and Ice Data center for providing Global Monthly EASE-Grid Snow Water Equivalent data,
534 National Oceanic and Atmospheric Administration for North American Regional Reanalysis
535 (NARR). We also acknowledge the World Climate Research Programme's Working Group on
536 Coupled Modeling Intercomparison Project CMIP5, and we thank the climate modeling groups
537 for producing and making available their model output. The data presented in this paper can be
538 accessed through our research website (<http://www.eaps.purdue.edu/ebdl/>)

539
540

541 **References:**

542 Allison, E. H., Perry, A. L., Badjeck, M.-C., Neil Adger, W., Brown, K., Conway, D., Halls, A.
543 S., Pilling, G. M., Reynolds, J. D., Andrew, N. L., and Dulvy, N. K.: Vulnerability of national
544 economies to the impacts of climate change on fisheries, *Fish and Fisheries*, 10, 173-196,
545 10.1111/j.1467-2979.2008.00310.x, 2009.
546 Allison, S. D., Wallenstein, M. D., and Bradford, M. A.: Soil-carbon response to warming
547 dependent on microbial physiology, *Nature Geoscience*, 3, 336-340, 10.1038/ngeo846, 2010.
548 Balser, T. C., Kinzig, A. P., and Firestone, M. K.: Linking soil microbial communities and
549 ecosystem functioning, *The functional consequences of biodiversity: Empirical progress and*
550 *theoretical extensions*, 265-293, 2002.
551 Blagodatskaya, E., and Kuzyakov, Y.: Active microorganisms in soil: Critical review of
552 estimation criteria and approaches, *Soil Biology and Biochemistry*, 67, 192-211,
553 10.1016/j.soilbio.2013.08.024, 2013.
554 Blagodatskaya, E., Khomyakov, N., Myachina, O., Bogomolova, I., Blagodatsky, S., and
555 Kuzyakov, Y.: Microbial interactions affect sources of priming induced by cellulose, *Soil*
556 *Biology and Biochemistry*, 74, 39-49, 10.1016/j.soilbio.2014.02.017, 2014.
557 Blagodatsky, S., Grote, R., Kiese, R., Werner, C., and Butterbach-Bahl, K.: Modelling of
558 microbial carbon and nitrogen turnover in soil with special emphasis on N-trace gases emission,
559 *Plant and soil*, 346, 297-330, 10.1007/s11104-011-0821-z, 2011.
560 Blagodatsky, S. A., Heinemeyer, O., and Richter, J.: Estimating the active and total soil
561 microbial biomass by kinetic respiration analysis, *Biol Fertil Soils*, 32, 73-81, 2000.
562 Bond-Lamberty, B., and Thomson, A.: Temperature-associated increases in the global soil
563 respiration record, *Nature*, 464, 579-582, 10.1038/nature08930, 2010.

564 Bond-Lamberty, B., Bailey, V. L., Chen, M., Gough, C. M., and Vargas, R.: Globally rising soil
565 heterotrophic respiration over recent decades, *Nature*, 560, 80-83, 10.1038/s41586-018-0358-x,
566 2018.

567 Bouskill, N. J., Tang, J., Riley, W. J., and Brodie, E. L.: Trait-based representation of biological
568 nitrification: model development, testing, and predicted community composition, *Frontiers in*
569 *microbiology*, 3, 364, 10.3389/fmicb.2012.00364, 2012.

570 Callaghan, T., Björn, L. O., Chernov, Y., Chapin, T., Christensen, T. R., Huntley, B., Ims, R.,
571 Jolly, D., Jonasson, S., Matveyeva, N., Panikov, N., Oechel, W., and Shaver, G.: Arctic tundra
572 and polar desert ecosystems, *Arctic climate impact assessment*, 243-352, 2005.

573 Carney, K. M., and Matson, P. A.: The influence of tropical plant diversity and composition on
574 soil microbial communities, *Microbial ecology*, 52, 226-238, 10.1007/s00248-006-9115-z, 2006.

575 Chmielewski, R. A. N., and Frank, J. F.: Formation of viable but nonculturable *Salmonella*
576 during starvation in chemically defined solutions, *Letters in Applied Microbiology*, 20, 380-384,
577 1995.

578 Classen, A. T., Sundqvist, M. K., Henning, J. A., Newman, G. S., Moore, J. A. M., Cregger, M.
579 A., Moorhead, L. C., and Patterson, C. M.: Direct and indirect effects of climate change on soil
580 microbial and soil microbial-plant interactions: What lies ahead?, *Ecosphere*, 6, art130,
581 10.1890/es15-00217.1, 2015.

582 Conant, R. T., Ryan, M. G., Ågren, G. I., Birge, H. E., Davidson, E. A., Eliasson, P. E., Evans, S.
583 E., Frey, S. D., Giardina, C. P., Hopkins, F. M., Hyvönen, R., Kirschbaum, M. U. F., Lavalley, J.
584 M., Leifeld, J., Parton, W. J., Megan Steinweg, J., Wallenstein, M. D., Martin Wetterstedt, J. Å.,
585 and Bradford, M. A.: Temperature and soil organic matter decomposition rates - synthesis of
586 current knowledge and a way forward, *Global change biology*, 17, 3392-3404, 10.1111/j.1365-
587 2486.2011.02496.x, 2011.

588 Coursolle, C., Margolis, H. A., Barr, A. G., Black, T. A., Amiro, B. D., McCaughey, J. H.,
589 Flanagan, L. B., Lafleur, P. M., Roulet, N. T., Bourque, C. P. A., Arain, M. A., Wofsy, S. C.,
590 Dunn, A., Morgenstern, K., Orchansky, A. L., Bernier, P. Y., Chen, J. M., Kidston, J., Saigusa,
591 N., and Hedstrom, N.: Late-summer carbon fluxes from Canadian forests and peatlands along an
592 east-west continental transect, *Canadian Journal of Forest Research*, 36, 783-800, 10.1139/x05-
593 270, 2006.

594 Davidson, E. A., Trumbore, S. E., and Amundson, R.: Biogeochemistry: soil warming and
595 organic carbon content, *Nature*, 408, 2000.

596 Davidson, E. A., and Janssens, I. A.: Temperature sensitivity of soil carbon decomposition and
597 feedbacks to climate change, *Nature*, 440, 165-173, 10.1038/nature04514, 2006.

598 Davidson, E. A., Janssens, I. A., and Luo, Y.: On the variability of respiration in terrestrial
599 ecosystems: moving beyond Q10, *Global change biology*, 12, 154-164, 10.1111/j.1365-
600 2486.2005.01065.x, 2006.

601 Davidson, E. A., Samanta, S., Caramori, S. S., and Savage, K.: The Dual Arrhenius and
602 Michaelis-Menten kinetics model for decomposition of soil organic matter at hourly to seasonal
603 time scales, *Global change biology*, 18, 371-384, 10.1111/j.1365-2486.2011.02546.x, 2012.

604 Duan, Q., Sorooshian, S., and Gupta, V. K.: Optimal use of the SCE-UA global optimization
605 method for calibrating watershed models, *Journal of Hydrology*, 158, 265-284, 1994.

606 Evans, S. E., and Wallenstein, M. D.: Soil microbial community response to drying and
607 rewetting stress: does historical precipitation regime matter?, *Biogeochemistry*, 109, 101-116,
608 10.1007/s10533-011-9638-3, 2011.

609 Fierer, N., Morse, J. L., Berthrong, S. T., Bernhardt, E. S., and Jackson, R. B.: Environmental
610 controls on the landscape - scale biogeography of stream bacterial communities, *Ecology*, 88,
611 2162-2173, 2007.

612 Frey, S. D., Lee, J., Melillo, J. M., and Six, J.: The temperature response of soil microbial
613 efficiency and its feedback to climate, *Nature Climate Change*, 3, 395-398,
614 10.1038/nclimate1796, 2013.

615 German, D. P., Marcelo, K. R. B., Stone, M. M., and Allison, S. D.: The Michaelis-Menten
616 kinetics of soil extracellular enzymes in response to temperature: a cross-latitudinal study,
617 *Global change biology*, 18, 1468-1479, 10.1111/j.1365-2486.2011.02615.x, 2012.

618 Gilmanov, T. G., Tieszen, L. L., Wylie, B. K., Flanagan, L. B., Frank, A. B., Haferkamp, M. R.,
619 Meyers, T. P., and Morgan, J. A.: Integration of CO₂ flux and remotely-sensed data for primary
620 production and ecosystem respiration analyses in the Northern Great Plains: potential for
621 quantitative spatial extrapolation, *Global Ecology and Biogeography*, 14, 271-292,
622 10.1111/j.1466-822X.2005.00151.x, 2005.

623 Gough, C. M., Hardiman, B. S., Nave, L. E., Bohrer, G., Maurer, K. D., Vogel, C. S.,
624 Nadelhoffer, K. J., and Curtis, P. S.: Sustained carbon uptake and storage following moderate
625 disturbance in a Great Lakes forest, *Ecological Applications*, 23, 1202-1215, 2013.

626 Goulden, M. L., Winston, G. C., McMillan, A. M. S., Litvak, M. E., Read, E. L., Rocha, A. V.,
627 and Rob Elliot, J.: An eddy covariance mesonet to measure the effect of forest age on
628 land-atmosphere exchange, *Global change biology*, 12, 2146-2162, 10.1111/j.1365-
629 2486.2006.01251.x, 2006.

630 Graham, E. B., Wieder, W. R., Leff, J. W., Weintraub, S. R., Townsend, A. R., Cleveland, C. C.,
631 Philippot, L., and Nemergut, D. R.: Do we need to understand microbial communities to predict
632 ecosystem function? A comparison of statistical models of nitrogen cycling processes, *Soil
633 Biology and Biochemistry*, 68, 279-282, 10.1016/j.soilbio.2013.08.023, 2014.

634 Graham, E. B., Knelman, J. E., Schindlbacher, A., Siciliano, S., Breulmann, M., Yannarell, A.,
635 Beman, J. M., Abell, G., Philippot, L., Prosser, J., Foulquier, A., Yuste, J. C., Glanville, H. C.,
636 Jones, D. L., Angel, R., Salminen, J., Newton, R. J., Burgmann, H., Ingram, L. J., Hamer, U.,
637 Siljanen, H. M., Peltoniemi, K., Potthast, K., Baneras, L., Hartmann, M., Banerjee, S., Yu, R. Q.,
638 Nogaro, G., Richter, A., Koranda, M., Castle, S. C., Goberna, M., Song, B., Chatterjee, A.,
639 Nunes, O. C., Lopes, A. R., Cao, Y., Kaisermann, A., Hallin, S., Strickland, M. S., Garcia-
640 Pausas, J., Barba, J., Kang, H., Isobe, K., Papaspyrou, S., Pastorelli, R., Lagomarsino, A.,
641 Lindstrom, E. S., Basiliko, N., and Nemergut, D. R.: Microbes as Engines of Ecosystem
642 Function: When Does Community Structure Enhance Predictions of Ecosystem Processes?,
643 *Frontiers in microbiology*, 7, 214, 10.3389/fmicb.2016.00214, 2016.

644 Griffis, T. J., Lee, X., Baker, J. M., Billmark, K., Schultz, N., Erickson, M., Zhang, X.,
645 Fassbinder, J., Xiao, W., and Hu, N.: Oxygen isotope composition of evapotranspiration and its
646 relation to C₄ photosynthetic discrimination, *Journal of Geophysical Research*, 116,
647 10.1029/2010jg001514, 2011.

648 Hagerty, S. B., van Groenigen, K. J., Allison, S. D., Hungate, B. A., Schwartz, E., Koch, G. W.,
649 Kolka, R. K., and Dijkstra, P.: Accelerated microbial turnover but constant growth efficiency
650 with warming in soil, *Nature Climate Change*, 4, 903-906, 10.1038/nclimate2361, 2014.

651 Hansen, J., Sato, M., Ruedy, R., Lo, K., Lea, D. W., and Medina-Elizade, M.: Global
652 temperature change, *Proceedings of the National Academy of Sciences of the United States of
653 America*, 103, 14288-14293, 10.1073/pnas.0606291103, 2006.

654 Harder, w., and Dijkhuizen, L.: Physiological responses to nutrient limitation, *Annual Review of*
655 *Microbiology*, 37, 1983.

656 Harris, I., Jones, P. D., Osborn, T. J., and Lister, D. H.: Updated high-resolution grids of monthly
657 climatic observations - the CRU TS3.10 Dataset, *International Journal of Climatology*, 34, 623-
658 642, 10.1002/joc.3711, 2014.

659 He, Y., Yang, J., Zhuang, Q., Harden, J. W., McGuire, A. D., Liu, Y., Wang, G., and Gu, L.:
660 Incorporating microbial dormancy dynamics into soil decomposition models to improve
661 quantification of soil carbon dynamics of northern temperate forests, *Journal of Geophysical*
662 *Research: Biogeosciences*, 120, 2596-2611, 10.1002/2015jg003130, 2015.

663 Hiller, R. V., McFadden, J. P., and Kljun, N.: Interpreting CO₂ Fluxes Over a Suburban Lawn:
664 The Influence of Traffic Emissions, *Boundary-Layer Meteorology*, 138, 215-230,
665 10.1007/s10546-010-9558-0, 2010.

666 Houghton, R. A.: Balancing the Global Carbon Budget, *Annual Review of Earth and Planetary*
667 *Sciences*, 35, 313-347, 10.1146/annurev.earth.35.031306.140057, 2007.

668 Hugelius, G., Strauss, J., Zubrzycki, S., Harden, J. W., Schuur, E. A. G., Ping, C. L.,
669 Schirmer, L., Grosse, G., Michaelson, G. J., Koven, C. D., and others, Donnell, J. A.,
670 Elberling, B., Mishra, U., Camill, P., Yu, Z., Palmtag, J., and Kuhry, P.: Estimated stocks of
671 circumpolar permafrost carbon with quantified uncertainty ranges and identified data gaps,
672 *Biogeosciences*, 11, 6573-6593, 10.5194/bg-11-6573-2014, 2014.

673 Jenkins, J. P., Richardson, A. D., Braswell, B. H., Ollinger, S. V., Hollinger, D. Y., and Smith,
674 M. L.: Refining light-use efficiency calculations for a deciduous forest canopy using
675 simultaneous tower-based carbon flux and radiometric measurements, *Agricultural and Forest*
676 *Meteorology*, 143, 64-79, 10.1016/j.agrformet.2006.11.008, 2007.

677 Kaiser, C., Franklin, O., Dieckmann, U., and Richter, A.: Microbial community dynamics
678 alleviate stoichiometric constraints during litter decay, *Ecology letters*, 17, 680-690,
679 10.1111/ele.12269, 2014.

680 Knorr, W., Prentice, I. C., House, J. I., and Holland, E. A.: Long-term sensitivity of soil carbon
681 turnover to warming, *Nature*, 433, 2005.

682 Lawrence, C. R., Neff, J. C., and Schimel, J. P.: Does adding microbial mechanisms of
683 decomposition improve soil organic matter models? A comparison of four models using data
684 from a pulsed rewetting experiment, *Soil Biology and Biochemistry*, 41, 1923-1934,
685 10.1016/j.soilbio.2009.06.016, 2009.

686 Lennon, J. T., and Jones, S. E.: Microbial seed banks: the ecological and evolutionary
687 implications of dormancy, *Nature reviews. Microbiology*, 9, 119-130, 10.1038/nrmicro2504,
688 2011.

689 Lloyd, A. H., Rupp, T. S., Fastie, C. L., and Starfield, A. M.: Patterns and dynamics of treeline
690 advance on the Seward Peninsula, Alaska, *Journal of Geophysical Research*, 108,
691 10.1029/2001jd000852, 2002.

692 Manzoni, S., Taylor, P., Richter, A., Porporato, A., and Agren, G. I.: Environmental and
693 stoichiometric controls on microbial carbon-use efficiency in soils, *The New phytologist*, 196,
694 79-91, 10.1111/j.1469-8137.2012.04225.x, 2012.

695 McEwing, K. R., Fisher, J. P., and Zona, D.: Environmental and vegetation controls on the
696 spatial variability of CH₄ emission from wet-sedge and tussock tundra ecosystems in the Arctic,
697 *Plant and soil*, 388, 37-52, 10.1007/s11104-014-2377-1, 2015.

698 McGuire, A. D., Melillo, J. M., Joyce, L. A., Kicklighter, D. W., Grace, A. L., III, B. M., and
699 Vorosmarty, C. J.: Interactions between carbon and nitrogen dynamics in estimating net primary

700 productivity for potential vegetation in North America, *Global Biogeochemical Cycles*, 6, 101-
701 124, 1992.

702 McGuire, A. D., Melillo, J. M., Kicklighter, D. W., and Joyce, L. A.: Equilibrium responses of
703 soil carbon to climate change: Empirical and process-based estimates, *Journal of Biogeography*,
704 22, 785-796, 1995.

705 McGuire, A. D., and Hobbie, J. E.: Global climate change and the equilibrium responses of
706 carbon storage in arctic and subarctic regions, In *Modeling the Arctic system: A workshop report*
707 *on the state of modeling in the Arctic System Science program*, 53-54, 1997.

708 McGuire, A. D., Anderson, L. G., Christensen, T. R., Dallimore, S., Guo, L., Hayes, D. J.,
709 Heimann, M., Lorenson, T. D., Macdonald, R. W., and Roulet, N.: Sensitivity of the carbon
710 cycle in the Arctic to climate change, *Ecological Monographs*, 79, 523-555, 2009.

711 McGuire, K. L., and Treseder, K. K.: Microbial communities and their relevance for ecosystem
712 models: Decomposition as a case study, *Soil Biology and Biochemistry*, 42, 529-535,
713 10.1016/j.soilbio.2009.11.016, 2010.

714 Me´tris, A., Gerrard, A. M., Cumming, R. H., Weigner, P., and Paca, J.: Modelling shock
715 loadings and starvation in the biofiltration of toluene and xylene, *Journal of Chemical*
716 *Technology and Biotechnology*, 76, 565-572, 2001.

717 Melillo, J. M., McGuire, A. D., Kicklighter, D. W., III, B. M., Vorosmarty, C. J., and Schloss, A.
718 L.: Global climate change and terrestrial net primary production, *Nature*, 363, 1993.

719 Melillo, J. M., Butler, S., Johnson, J., Mohan, J., Steudler, P., Lux, H., Burrows, E., Bowles, F.,
720 Smith, R., Scott, L., Vario, C., Hill, T., Burton, A., Zhou, Y.-M., and Tang, J.: Soil warming,
721 carbon - nitrogen interactions, and forest carbon budgets, *PNAS*, 108, 9508-9512, 2011.

722 Merbold, L., Kutsch, W. L., Corradi, C., Kolle, O., Rebmann, C., Stoy, P. C., Zimov, S. A., and
723 Schulze, E. D.: Artificial drainage and associated carbon fluxes (CO₂/CH₄) in a tundra
724 ecosystem, *Global change biology*, 15, 2599-2614, 10.1111/j.1365-2486.2009.01962.x, 2009.

725 Moorhead, D. L., and Sinsabaugh, R. L.: A theoretical model of litter decay and microbial
726 interaction, *Ecological Monographs*, 76, 151-174, 2006.

727 Oechel, W. C., Laskowski, C. A., Burba, G., Gioli, B., and Kalhori, A. A. M.: Annual patterns
728 and budget of CO₂ flux in an Arctic tussock tundra ecosystem, *Journal of Geophysical Research:*
729 *Biogeosciences*, 119, 323-339, 10.1002/2013jg002431, 2014.

730 P.J. Hanson, N. T. E., C.T. Garten, J.A. Andrews: Separating root and soil microbial
731 contributions to soil respiration: A review of methods and observations, *Biogeochemistry*, 48,
732 115-146, 2000.

733 Parton, W. J., Scurlock, J. M. O., Ojima, D. S., Gilmanov, T. G., Scholes, R. J., Schimel, D. S.,
734 Kirchner, T., Menaut, J. C., Seastedt, T., Moya, E. G., Kamnalrut, A., and Kinyamario, J. I.:
735 Observations and modeling of biomass and soil organic matter dynamics for the grassland biome
736 worldwide, *Global Biogeochemical Cycles*, 7, 785-809, 1993.

737 Raich, J. W., Rastetter, E. B., Melillo, J. M., Kicklighter, D. W., Steudler, P. A., Peterson, B. J.,
738 Grace, A. L., III, B. M., and Vorosmarty, C. J.: Potential net primary productivity in South
739 America: application of a global model, *Ecological Applications*, 1, 399-429, 1991.

740 Richardson, A. D., Jenkins, J. P., Braswell, B. H., Hollinger, D. Y., Ollinger, S. V., and Smith,
741 M. L.: Use of digital webcam images to track spring green-up in a deciduous broadleaf forest,
742 *Oecologia*, 152, 323-334, 10.1007/s00442-006-0657-z, 2007.

743 Running, S. W., and Coughlan, J. C.: A general model of forest ecosystem processes for regional
744 applications I. Hydrologic balance, canopy gas exchange and primary production processes.,
745 *Ecological Modelling*, 42, 125-154, 1988.

746 Schimel, D. S.: Terrestrial ecosystems and the carbon cycle, *Global change biology*, 1, 77-91,
747 1995.

748 Schimel, D. S., House, J. I., Hibbard, K. A., Bousquet, P., Ciais, P., Peylin, P., Braswell, B. H.,
749 Apps, M. J., Baker, D., Bondeau, A., Canadell, J., Churkina, G., Cramer, W., Denning, A. S.,
750 Field, C. B., Friedlingstein, P., Goodale, C., Heimann, M., Houghton, R. A., Melillo, J. M., III,
751 B. M., Murdiyarso, D., Noble, I., Pacala, S. W., Prentice, I. C., Raupach, M. R., Rayner, P. J.,
752 Scholes, R. J., Steffen, W. L., and Wirth, C.: Recent patterns and mechanisms of carbon
753 exchange by terrestrial ecosystems, *Nature*, 414, 2001.

754 Schimel, J.: Microbes and global carbon, *Nature Climate Change*, 3, 867-868,
755 10.1038/nclimate2015, 2013.

756 Schimel, J. P., and Weintraub, M. N.: The implications of exoenzyme activity on microbial
757 carbon and nitrogen limitation in soil: a theoretical model, *Soil Biology and Biochemistry*, 35,
758 549-563, 10.1016/s0038-0717(03)00015-4, 2003.

759 Schimel, J. P., and Schaeffer, S. M.: Microbial control over carbon cycling in soil, *Frontiers in*
760 *microbiology*, 3, 348, 10.3389/fmicb.2012.00348, 2012.

761 Schlesinger, W. H., and Andrews, J. A.: Soil respiration and the global carbon cycle,
762 *Biogeochemistry*, 48, 7-20, 2000.

763 Schmidt, M. W., Torn, M. S., Abiven, S., Dittmar, T., Guggenberger, G., Janssens, I. A., Kleber,
764 M., Kogel-Knabner, I., Lehmann, J., Manning, D. A., Nannipieri, P., Rasse, D. P., Weiner, S.,
765 and Trumbore, S. E.: Persistence of soil organic matter as an ecosystem property, *Nature*, 478,
766 49-56, 10.1038/nature10386, 2011.

767 Serreze, M. C., and Francis, J. A.: The Arctic on the fast track of change, *Weather*, 61, 65-69,
768 2006.

769 Stolpovsky, K., Martinez-Lavanchy, P., Heipieper, H. J., Van Cappellen, P., and Thullner, M.:
770 Incorporating dormancy in dynamic microbial community models, *Ecological Modelling*, 222,
771 3092-3102, 10.1016/j.ecolmodel.2011.07.006, 2011.

772 Stow, D. A., Hope, A., McGuire, D., Verbyla, D., Gamon, J., Huemmrich, F., Houston, S.,
773 Racine, C., Sturm, M., Tape, K., Hinzman, L., Yoshikawa, K., Tweedie, C., Noyle, B.,
774 Silapaswan, C., Douglas, D., Griffith, B., Jia, G., Epstein, H., Walker, D., Daeschner, S.,
775 Petersen, A., Zhou, L., and Myneni, R.: Remote sensing of vegetation and land-cover change in
776 Arctic Tundra Ecosystems, *Remote Sensing of Environment*, 89, 281-308,
777 10.1016/j.rse.2003.10.018, 2004.

778 Strickland, M. S., Lauber, C., Fierer, N., and Bradford, M. A.: Testing the functional
779 significance of microbial community composition, *Ecology*, 90, 441-451, 2009.

780 Tang, J., Q. Zhuang (2009) A global sensitivity analysis and Bayesian inference framework for
781 improving the parameter estimation and prediction of a process-based Terrestrial Ecosystem
782 Model *J. Geophys. Res.*, 114, D15303, doi:10.1029/2009JD011724., 2009.

783 Tang, J., Q. Zhuang (2008) Equifinality in parameterization of process-based biogeochemistry
784 models: A significant uncertainty source to the estimation of regional carbon dynamics *J.*
785 *Geophys. Res.*, 113, G04010, doi:10.1029/2008JG000757, 2008.

786 Tang, J., and Riley, W. J.: Weaker soil carbon–climate feedbacks resulting from microbial and
787 abiotic interactions, *Nature Climate Change*, 5, 56-60, 10.1038/nclimate2438, 2014.

788 Tape, K. E. N., Sturm, M., and Racine, C.: The evidence for shrub expansion in Northern Alaska
789 and the Pan-Arctic, *Global change biology*, 12, 686-702, 10.1111/j.1365-2486.2006.01128.x,
790 2006.

791 Tarnocai, C., Canadell, J. G., Schuur, E. A. G., Kuhry, P., Mazhitova, G., and Zimov, S.: Soil
792 organic carbon pools in the northern circumpolar permafrost region, *Global Biogeochemical*
793 *Cycles*, 23, n/a-n/a, 10.1029/2008gb003327, 2009.

794 Thullner, M., Van Cappellen, P., and Regnier, P.: Modeling the impact of microbial activity on
795 redox dynamics in porous media, *Geochimica et Cosmochimica Acta*, 69, 5005-5019,
796 10.1016/j.gca.2005.04.026, 2005.

797 Todd-Brown, K. E. O., Hopkins, F. M., Kivlin, S. N., Talbot, J. M., and Allison, S. D.: A
798 framework for representing microbial decomposition in coupled climate models,
799 *Biogeochemistry*, 109, 19-33, 10.1007/s10533-011-9635-6, 2011.

800 Todd-Brown, K. E. O., Randerson, J. T., Post, W. M., Hoffman, F. M., Tarnocai, C., Schuur, E.
801 A. G., and Allison, S. D.: Causes of variation in soil carbon simulations from CMIP5 Earth
802 system models and comparison with observations, *Biogeosciences*, 10, 1717-1736, 10.5194/bg-
803 10-1717-2013, 2013.

804 Treseder, K. K., Balsler, T. C., Bradford, M. A., Brodie, E. L., Dubinsky, E. A., Eviner, V. T.,
805 Hofmockel, K. S., Lennon, J. T., Levine, U. Y., MacGregor, B. J., Pett-Ridge, J., and Waldrop,
806 M. P.: Integrating microbial ecology into ecosystem models: challenges and priorities,
807 *Biogeochemistry*, 109, 7-18, 10.1007/s10533-011-9636-5, 2011.

808 W. D. Billings, K. M. P., G. R. Shaver, A. W. Trent: Root Growth, Respiration, and Carbon
809 Dioxide Evolution in an Arctic Tundra Soil, *Arctic and Alpine Research*, 9, 129-137,
810 10.1080/00040851.1977.12003908, 1977.

811 Wang, G., M. A. M., Lianhong Gu, Christopher W. Schadt: Representation of Dormant and
812 Active Microbial Dynamics for Ecosystem Modeling, *Public Library of Science*, 9,
813 10.1371/journal.pone.0089252.g001, 2014.

814 Wang, G., Jagadamma, S., Mayes, M. A., Schadt, C. W., Steinweg, J. M., Gu, L., and Post, W.
815 M.: Microbial dormancy improves development and experimental validation of ecosystem
816 model, *The ISME journal*, 9, 226-237, 10.1038/ismej.2014.120, 2015.

817 Wang Wei, F. J., T. Oikawa: Contribution of Root and Microbial Respiration to Soil CO₂ Efflux
818 and Their Environmental Controls in a Humid Temperate Grassland of Japan, *Pedosphere*, 19,
819 31-39, 2009.

820 Werf, H. V. d., and Verstraete, W.: Estimation of active soil microbial biomass by mathematical
821 analysis of respiration curves: relation to conventional estimation of total biomass, *Soil Biology*
822 *and Biochemistry*, 19, 267-271, 1987.

823 White, A., Cannell, M. G. R., and Friend, A. D.: The high-latitude terrestrial carbon sink: a
824 model analysis *Global change biology*, 6, 227-245, 2000.

825 Wieder, W. R., Bonan, G. B., and Allison, S. D.: Global soil carbon projections are improved by
826 modelling microbial processes, *Nature Climate Change*, 3, 909-912, 10.1038/nclimate1951,
827 2013.

828 Xu, X., Schimel, J. P., Thornton, P. E., Song, X., Yuan, F., and Goswami, S.: Substrate and
829 environmental controls on microbial assimilation of soil organic carbon: a framework for Earth
830 system models, *Ecology letters*, 17, 547-555, 10.1111/ele.12254, 2014.

831 Zha, J., and Zhuang, Q.: Microbial decomposition processes and vulnerable arctic soil organic
832 carbon in the 21st century, *Biogeosciences*, 15, 5621-5634, 10.5194/bg-15-5621-2018, 2018a.

833 Zha, J., and Zhuang, Q.: Microbial decomposition processes and vulnerable Arctic soil organic
834 carbon in the 21st century, *Biogeosciences Discussions*, 1-34, 10.5194/bg-2018-241, 2018b.

835 Zhou, L., Tucker, C. J., Kaufmann, R. K., Slayback, D., Shabanov, N. V., and Myneni, R. B.:
836 Variations in northern vegetation activity inferred from satellite data of vegetation index during

837 1981 to 1999, *Journal of Geophysical Research: Atmospheres*, 106, 20069-20083,
838 10.1029/2000jd000115, 2001.

839 Zhuang, Q., Romanovsky, V. E., and McGuire, A. D.: Incorporation of a permafrost model into a
840 large-scale ecosystem model: Evaluation of temporal and spatial scaling issues in simulating soil
841 thermal dynamics, *Journal of Geophysical Research: Atmospheres*, 106, 33649-33670,
842 10.1029/2001jd900151, 2001.

843 Zhuang, Q., McGuire, A. D., O'Neill, K. P., Harden, J. W., Romanovsky, V. E., and Yarie, J.:
844 Modeling soil thermal and carbon dynamics of a fire chronosequence in interior Alaska, *Journal*
845 *of Geophysical Research*, 108, 10.1029/2001jd001244, 2002.

846 Zhuang, Q., He, J., Lu, Y., Ji, L., Xiao, J., and Luo, T.: Carbon dynamics of terrestrial
847 ecosystems on the Tibetan Plateau during the 20th century: an analysis with a process-based
848 biogeochemical model, *Global Ecology and Biogeography*, 19, 649-662, 10.1111/j.1466-
849 8238.2010.00559.x, 2010.

850 Zhuang, Q., Zhu, X., He, Y., Prigent, C., Melillo, J. M., David McGuire, A., Prinn, R. G., and
851 Kicklighter, D. W.: Influence of changes in wetland inundation extent on net fluxes of carbon
852 dioxide and methane in northern high latitudes from 1993 to 2004, *Environmental Research*
853 *Letters*, 10, 095009, 10.1088/1748-9326/10/9/095009, 2015.

854 Zhuang, Q., McGuire, A. D., Melillo, J. M., Clein, J. S., Dargaville, R. J., Kicklighter, D. W.,
855 Myneni, R. B., Dong, J., Romanovsky, V. E., Harden, J., and Hobbie, J. E.: Carbon cycling in
856 extratropical terrestrial ecosystems of the Northern Hemisphere during the 20th century: a
857 modeling analysis of the influences of soil thermal dynamics, *Tellus B: Chemical and Physical*
858 *Meteorology*, 55, 751-776, 10.3402/tellusb.v55i3.16368, 2016.

859
860
861
862

863

864 **Author contributions.** Q.Z. designed the study. J.Z. conducted model development, simulation
865 and analysis. J.Z. and Q. Z. wrote the paper.

866 **Competing financial interests.** The submission has no competing financial interests.

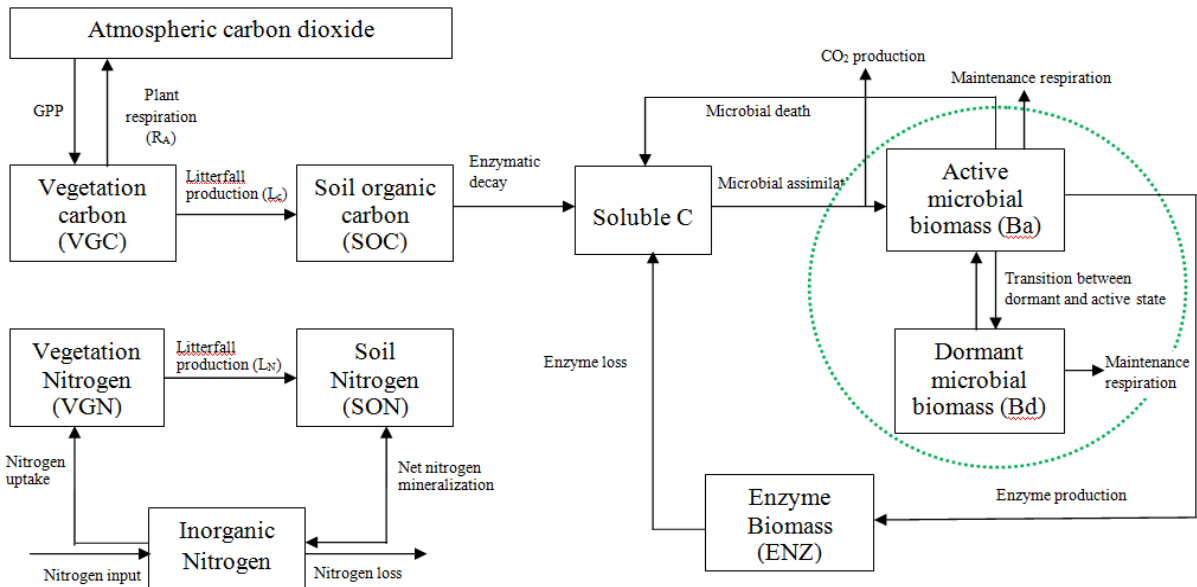
867 **Materials & Correspondence.** Correspondence and material requests should be addressed to
868 qzhuang@purdue.edu.

869

870

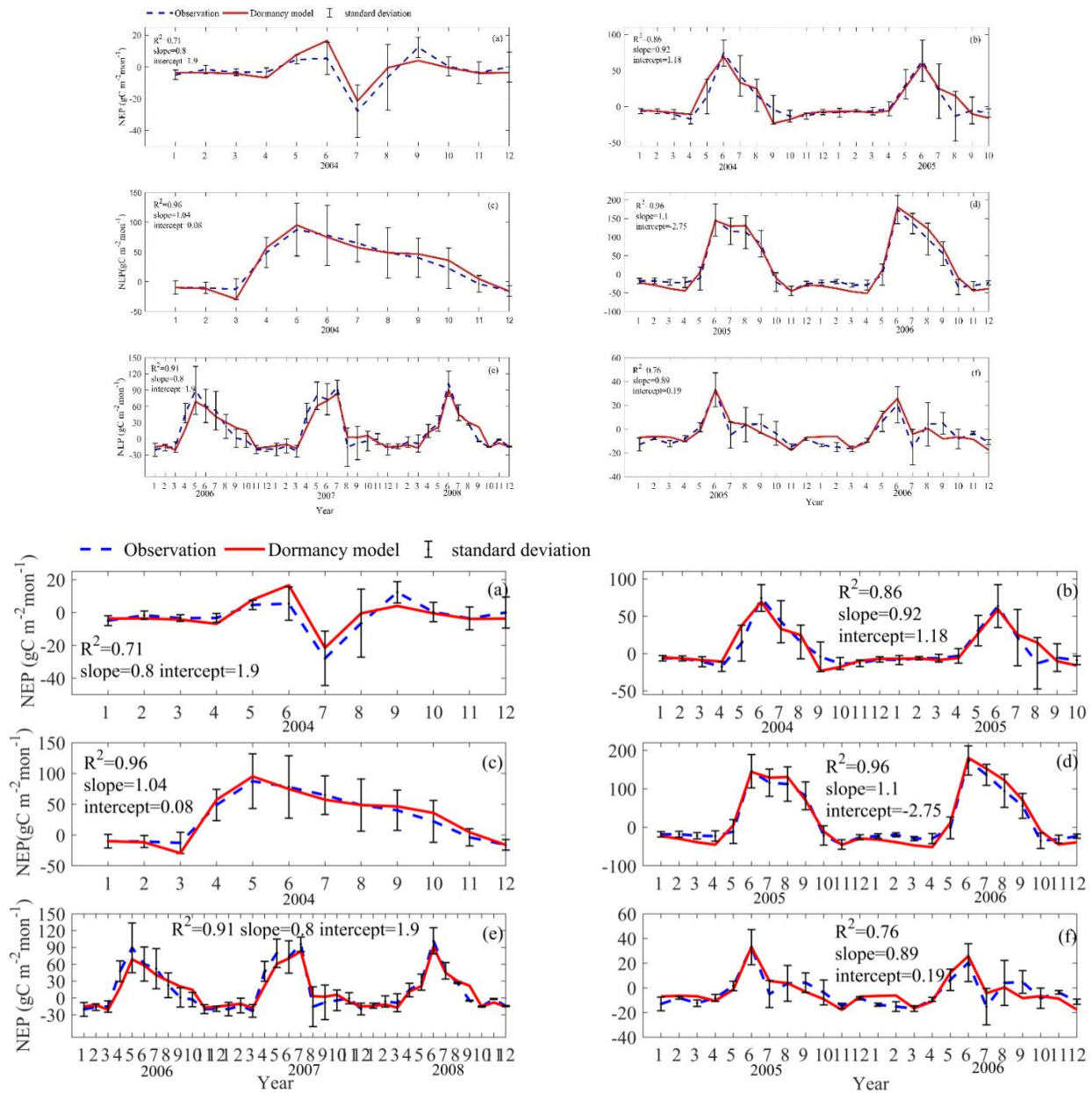
871

872



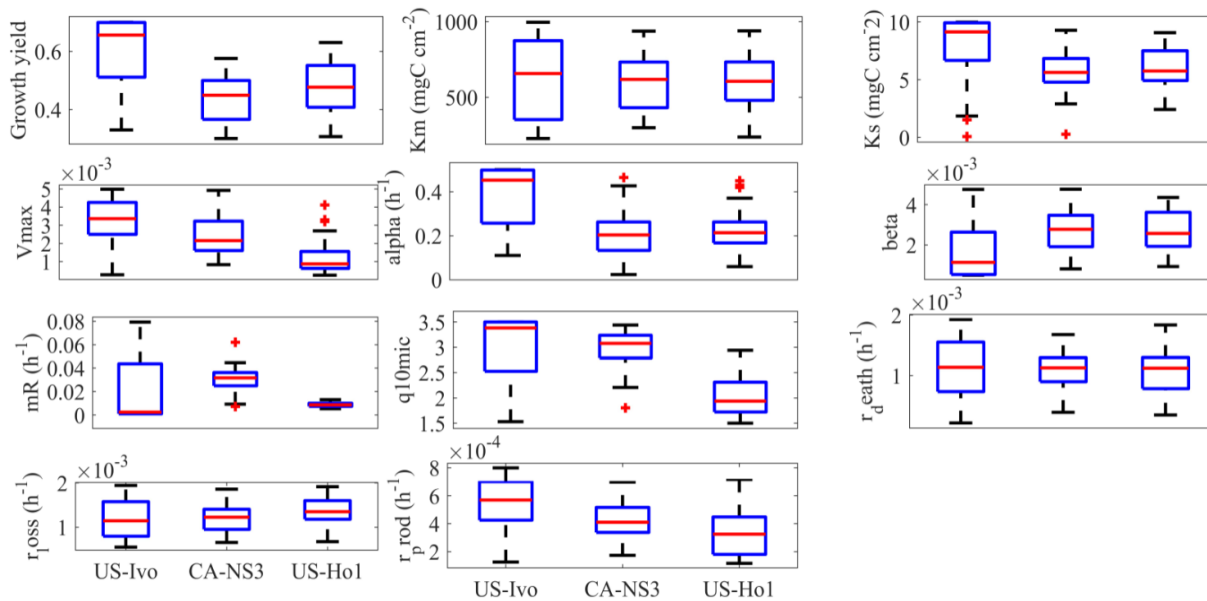
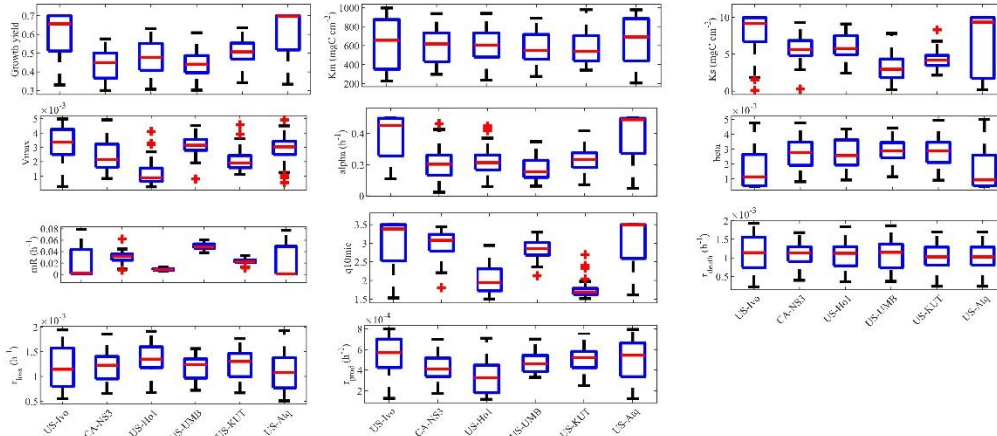
873
 874 Figure 1. Framework of the dormancy model: microbial biomass is split into two parts, active
 875 microbial biomass and dormant microbial biomass (shown in the green dashed circle).
 876 Maintenance respiration from these two parts, and the CO₂ production through microbial
 877 assimilation contributes to heterotrophic respiration. The model was revised based on Zha &
 878 Zhuang (2018).
 879

880

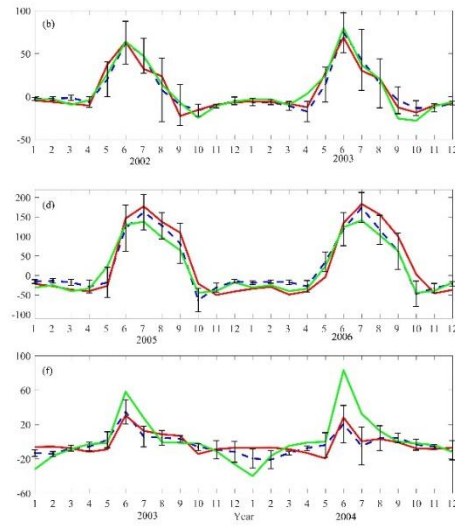
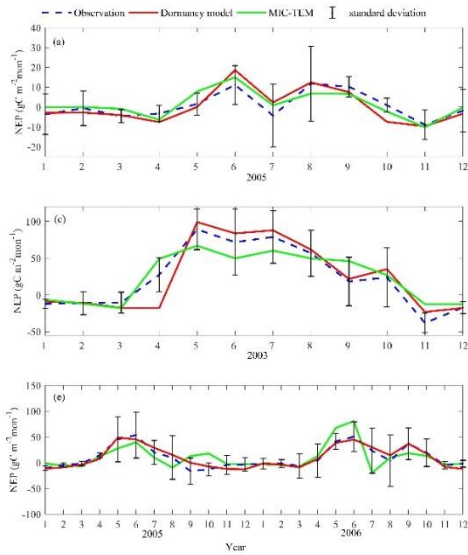


881

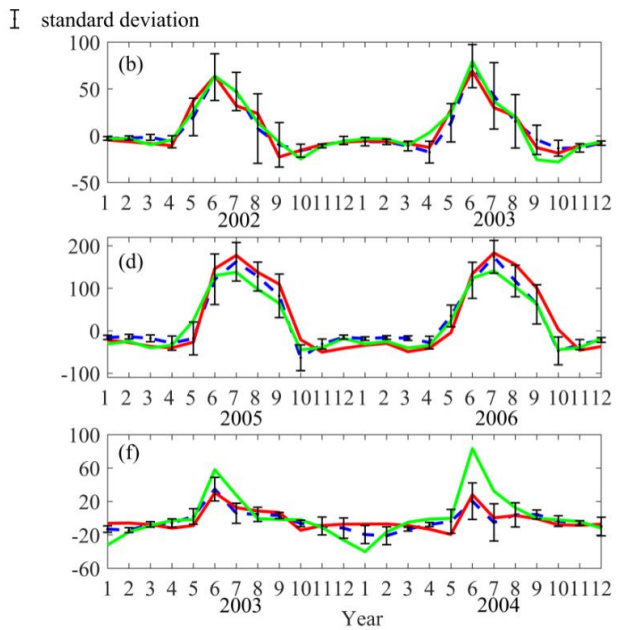
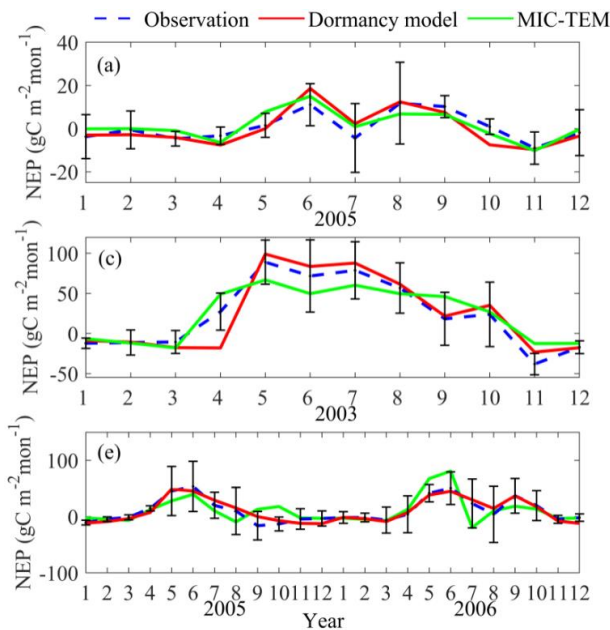
882 Figure 2. Comparison between observed and simulated NEP ($\text{gC m}^{-2} \text{mon}^{-1}$) at: (a) Ivotuk (alpine
 883 tundra), (b) UCI-1964 burn site (boreal forest), (c) Howland Forest (main tower) (temperate
 884 coniferous forest), (d) Univ. of Mich. Biological Station (Temperate deciduous forest), (e)
 885 KUOM Turfgrass Field (Grassland), and (f) Atqasuk (Wet tundra). Note: scales are different.
 886 Error bars represent standard errors among daily measure data in one month.
 887



891 Figure 3. Boxplot of parameter posterior distribution that are obtained after ensemble inverse
 892 modeling for MIC-TEM-dormancy all six sites: US-Ivo: Iivotuk (alpine tundra), CA-NS3: UCI-
 893 1964 burn site (boreal forest), US-Ho1: Howland Forest (temperate coniferous forest), US-UMB:
 894 Univ. of Mich. Biological Station (temperate deciduous forest), US-KUT: KUOM Turfgrass
 895 Field (grassland), US-Atq: Atqasuk (wet tundra).



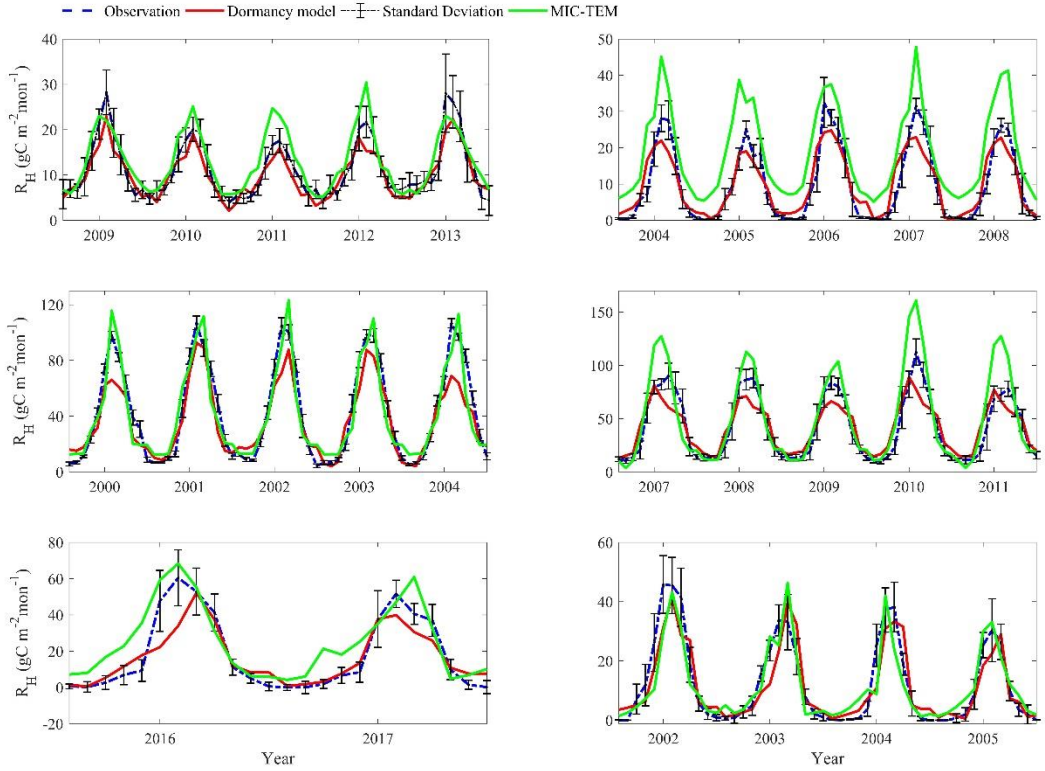
897



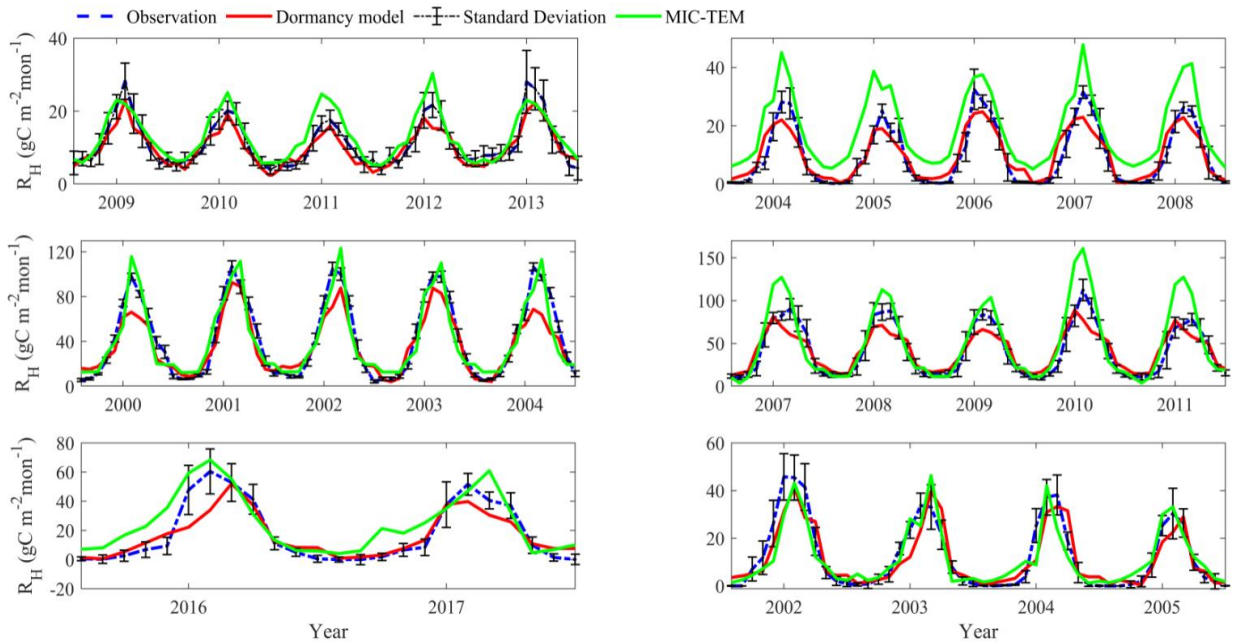
898

899 Figure 4. Comparison between observed and simulated NEP ($\text{gC m}^{-2}\text{mon}^{-1}$) at: (a) Igotuk (alpine
900 tundra), (b) UCI-1964 burn site (boreal forest), (c) Howland Forest (main tower) (temperate
901 coniferous forest), (d) Bartlett Experimental Forest (Temperate deciduous forest), (e) Brookings
902 (Grassland), and (f) Atqasuk (Wet tundra). Note: scales are different.

903

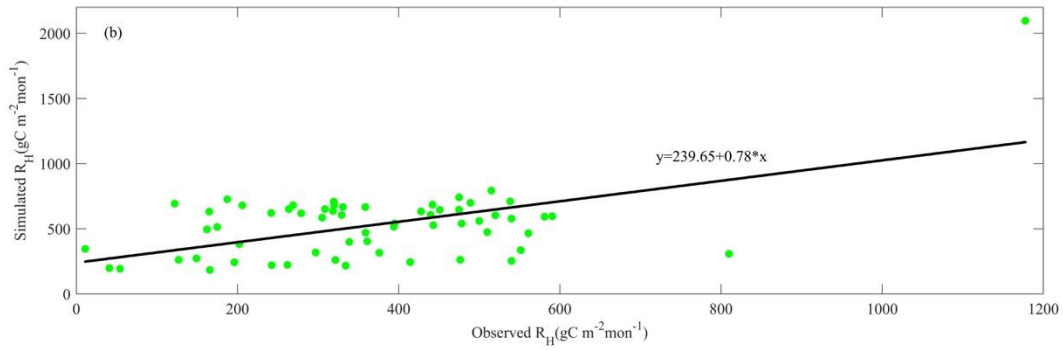
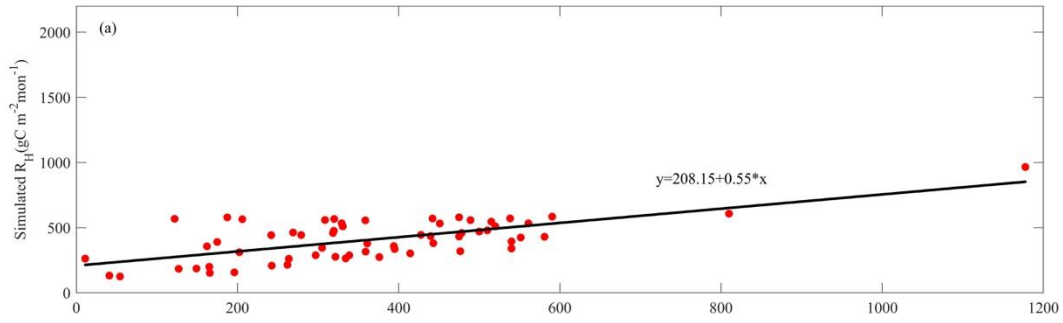


904

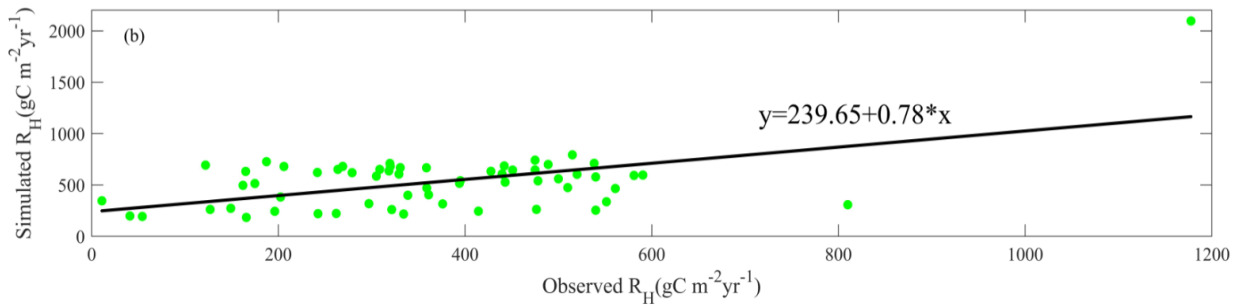
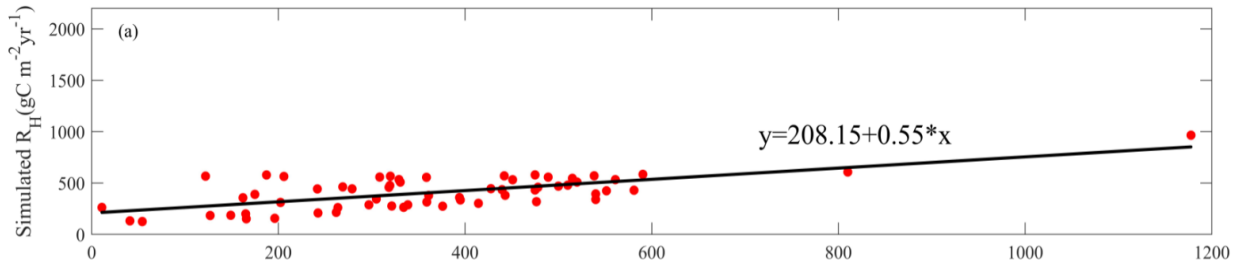


905

906 Figure 5. Comparison between observed and simulated R_H (gC m⁻² mon⁻¹) at: (a) US-EML (alpine
 907 tundra), (b) CA-SJ2 (boreal forest), (c) US-Ho2 (temperate coniferous forest), (d) US-UMB
 908 (Temperate deciduous forest), (e) US-Ro4 (Grassland), and (f) RU-Che (Wet tundra). Note:
 909 scales are different.



910

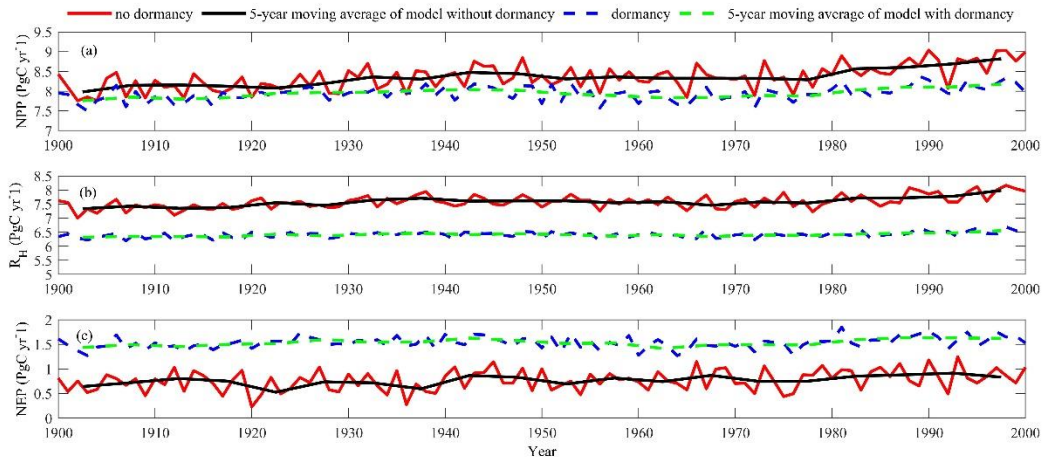


911

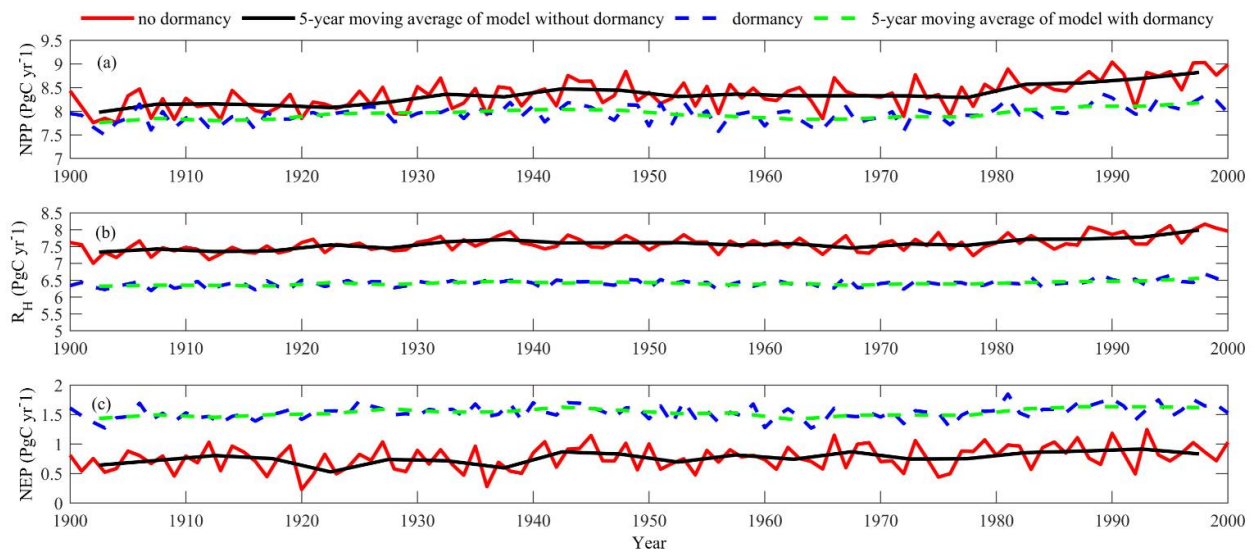
912 Figure 6. Linear regression between simulated and observed annual R_H ($\text{gC m}^{-2}\text{yr}^{-1}$) for: (a) MIC-
 913 TEM-dormancy, and (b) MIC-TEM.

914

915

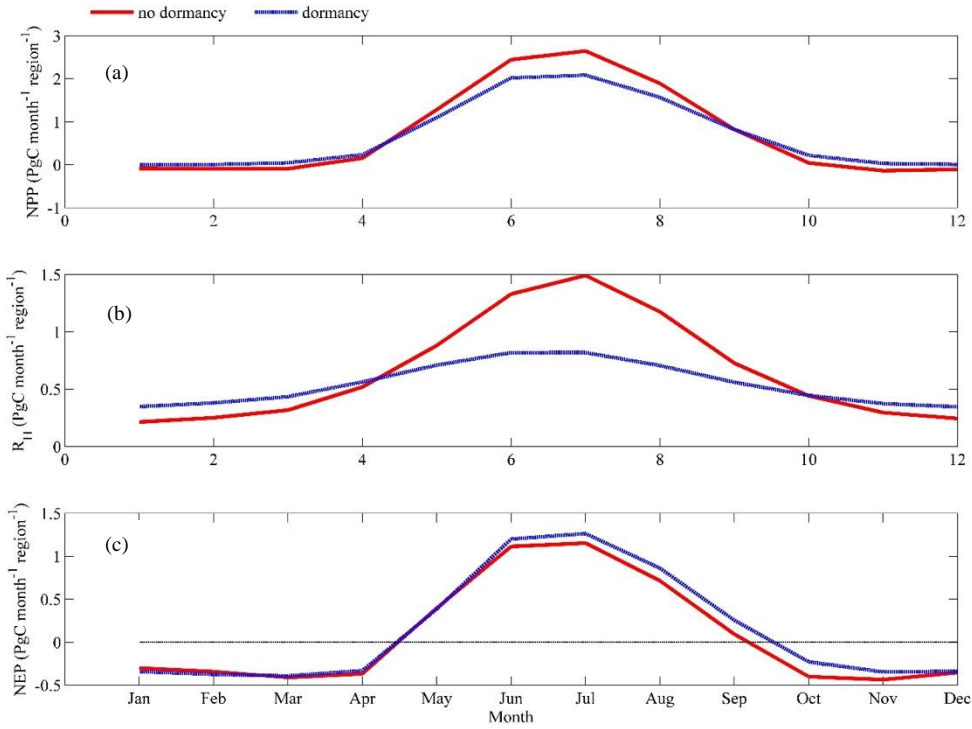


916

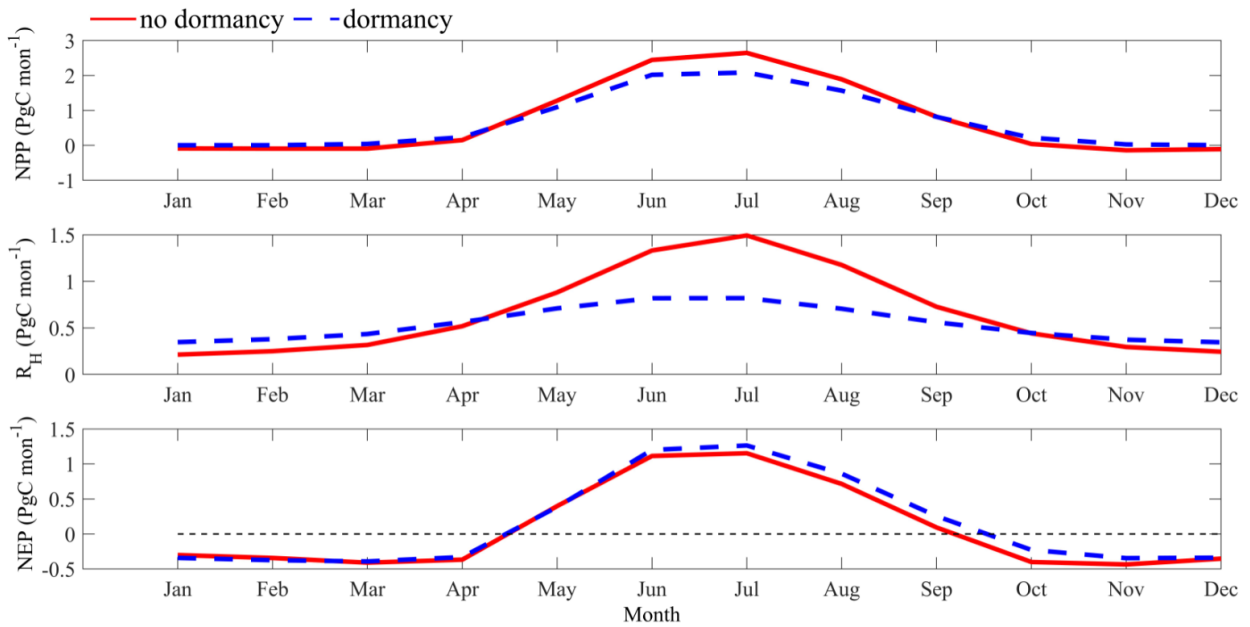


917

918 Figure 7. Simulated annual net primary production (NPP, top panel), heterotrophic respiration (R_H ,
 919 center panel) and net ecosystem production (NEP, bottom panel) during the 20th century by
 920 dormancy model and MIC-TEM, respectively.

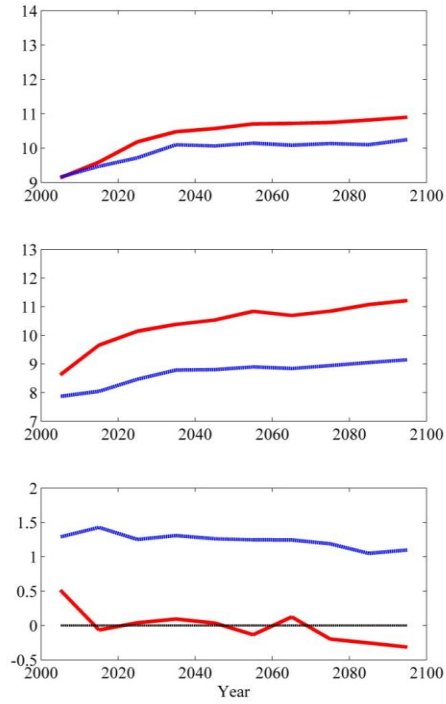
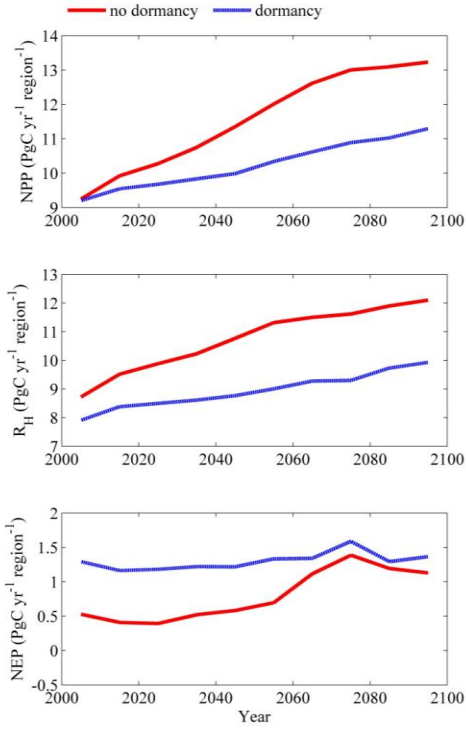


921

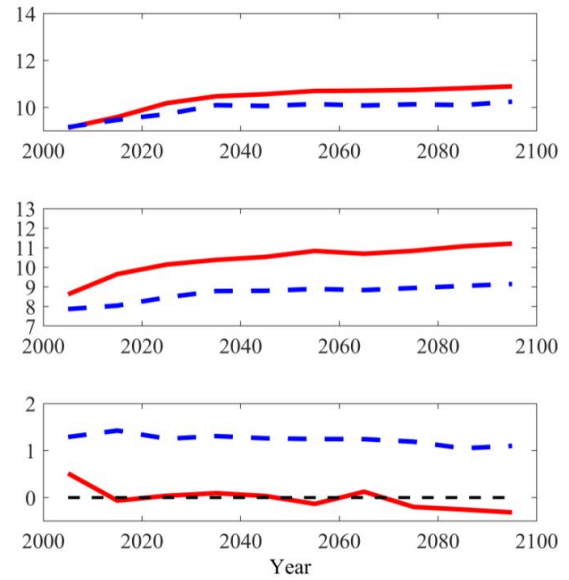
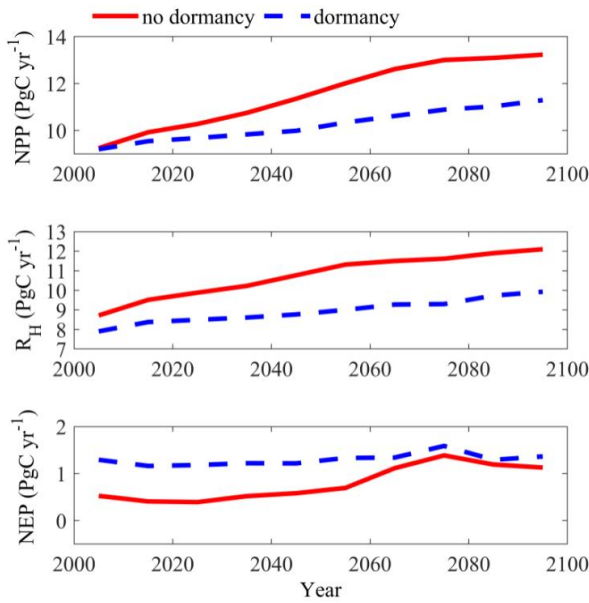


922

923 Figure 8. Annual seasonal pattern of simulated (a) net primary production (NPP, top panel),
 924 heterotrophic respiration (R_H , center panel) and (c) net ecosystem production (NEP, bottom
 925 panel) during the 1990s from dormancy model and MIC-TEM.



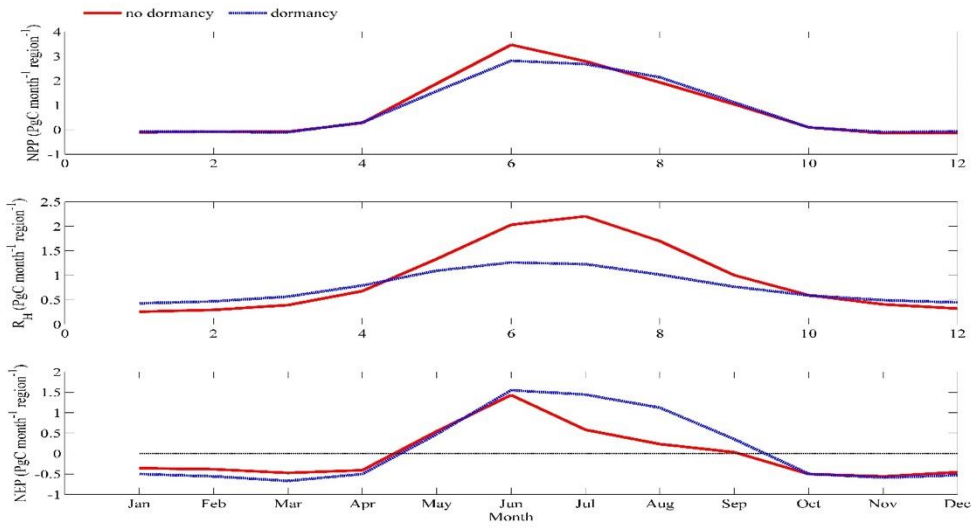
926



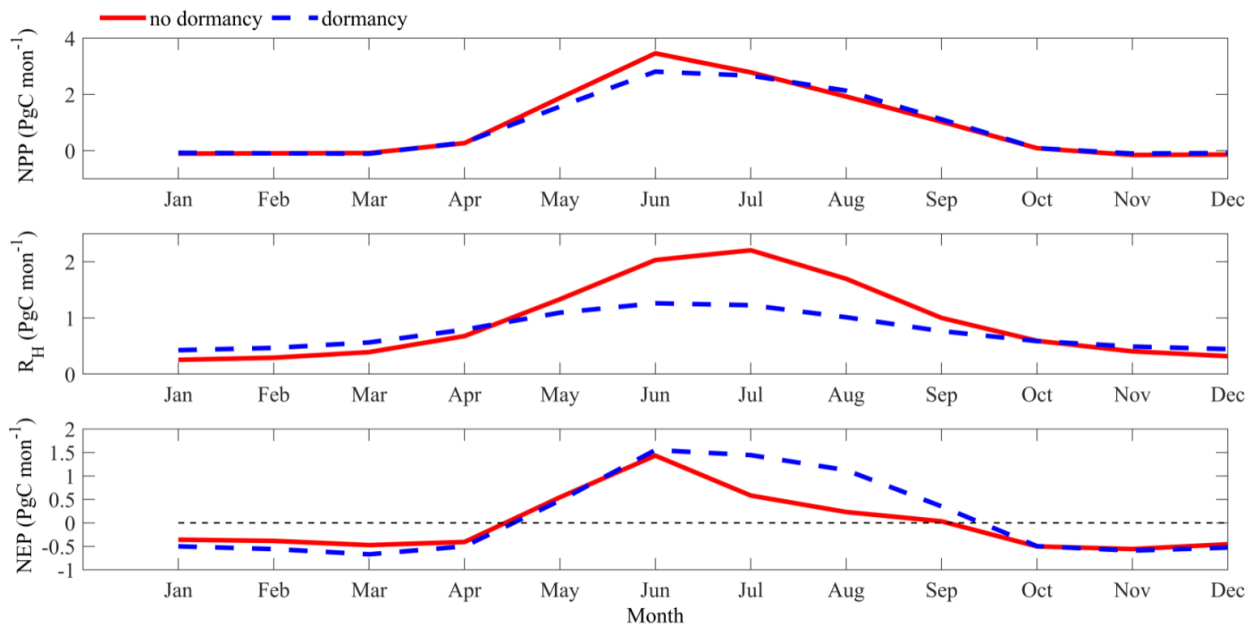
927

928 Figure 9. Predicted changes in carbon fluxes: (i) NPP, (ii) R_H , and (iii) NEP for all land areas north
 929 of 45 °N in response to transient climate change under the RCP 8.5 scenario (left panel) and RCP
 930 2.6 scenario (right panel) with dormancy model and MIC-TEM, respectively. The decadal running
 931 mean is applied.
 932
 933

934 (a)

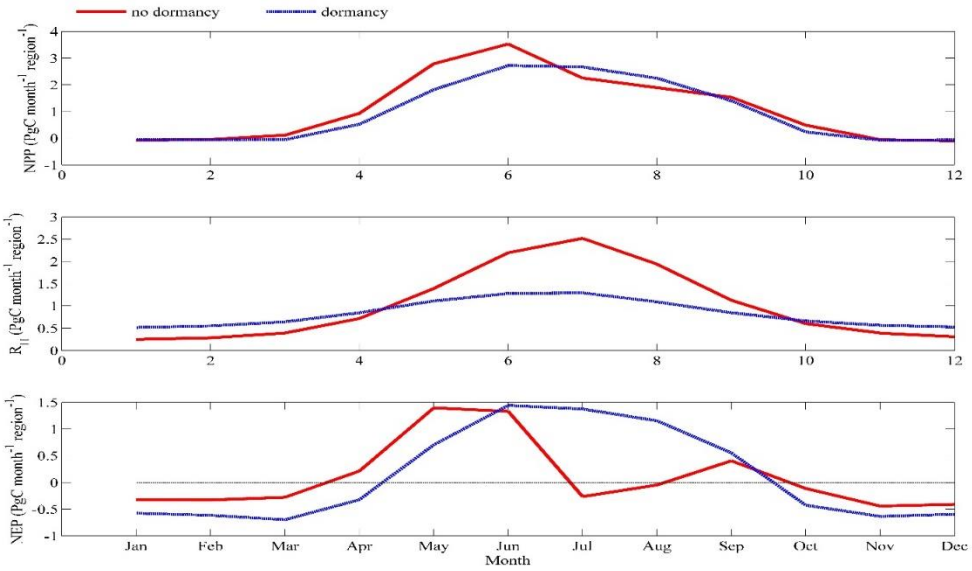


935

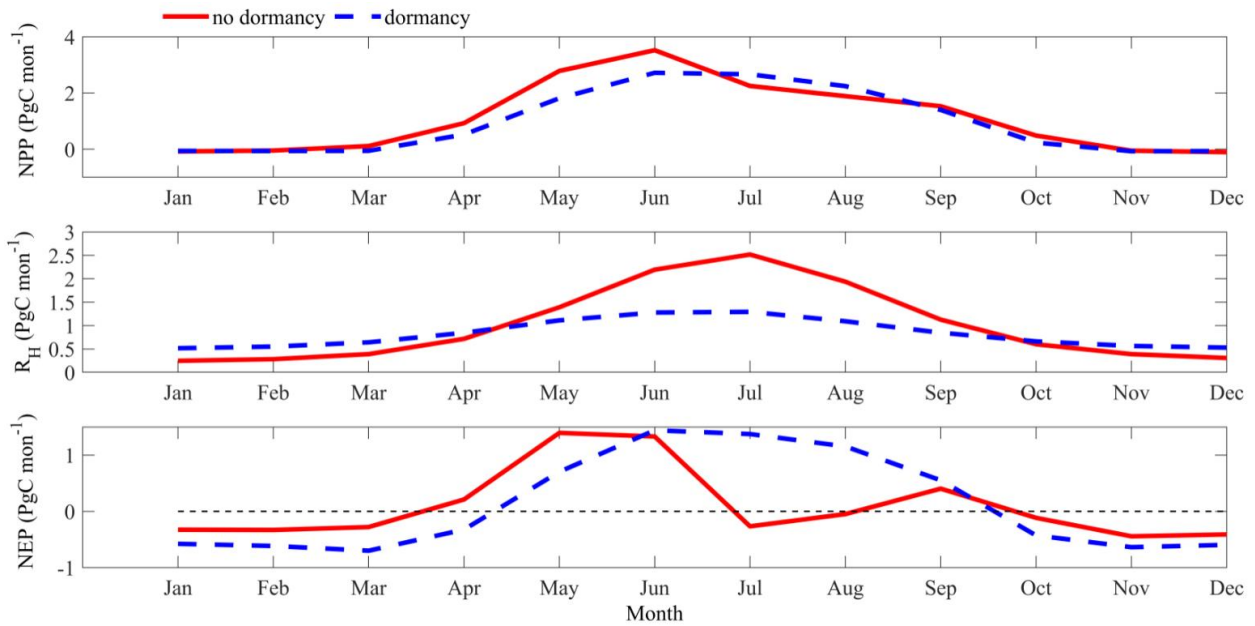


936

937 (b)



938

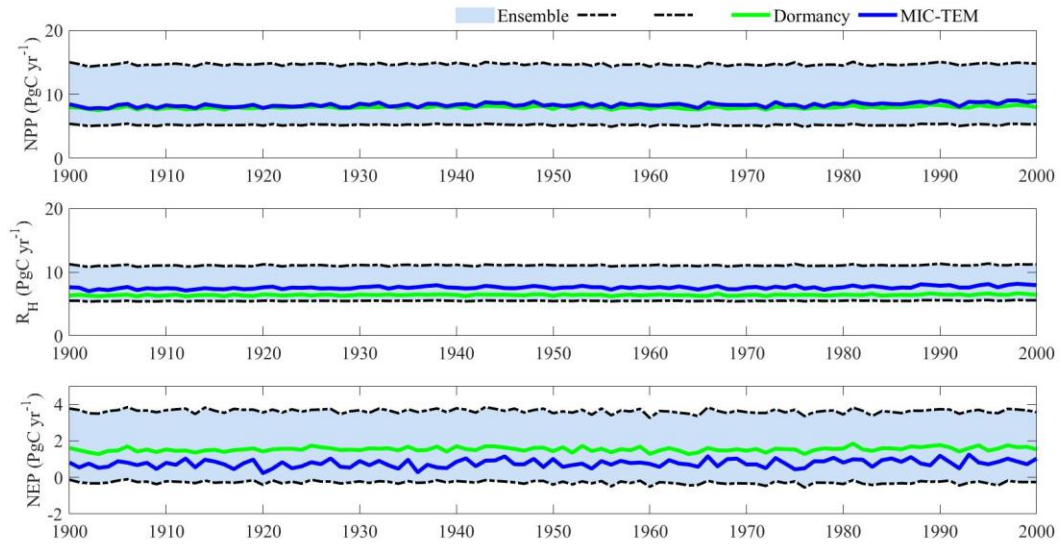


939

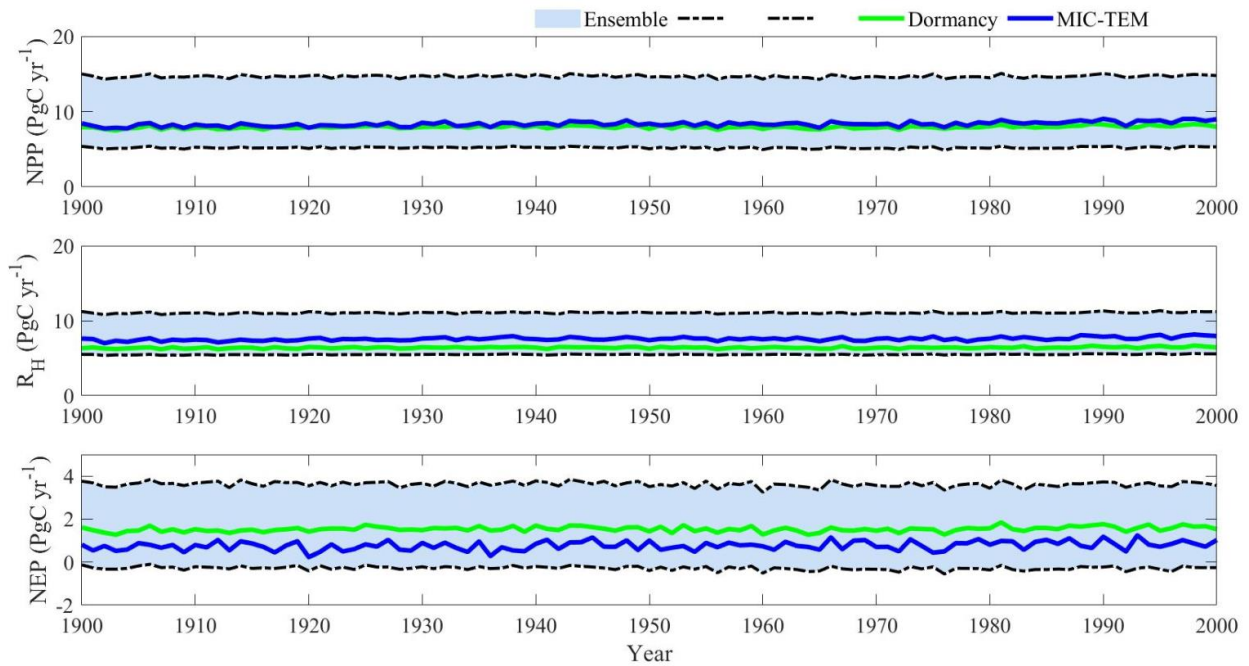
940 Figure 10. Annual seasonal pattern of simulated net primary production (NPP, top panel),
 941 heterotrophic respiration (R_H , center panel) and net ecosystem production (NEP, bottom panel)
 942 during the 2090s from dormancy model and MIC-TEM under: (a) RCP 2.6 scenario (top panel)
 943 and (b) RCP 8.5 scenario (bottom panel).
 944

945

946



947



948

949

950 Figure 11. Simulated annual net primary production (NPP, top panel), heterotrophic respiration
 951 (R_H , center panel) and net ecosystem production (NEP, bottom panel) by MIC-TEM-dormancy
 952 with ensemble of parameters.

953

954

955

956

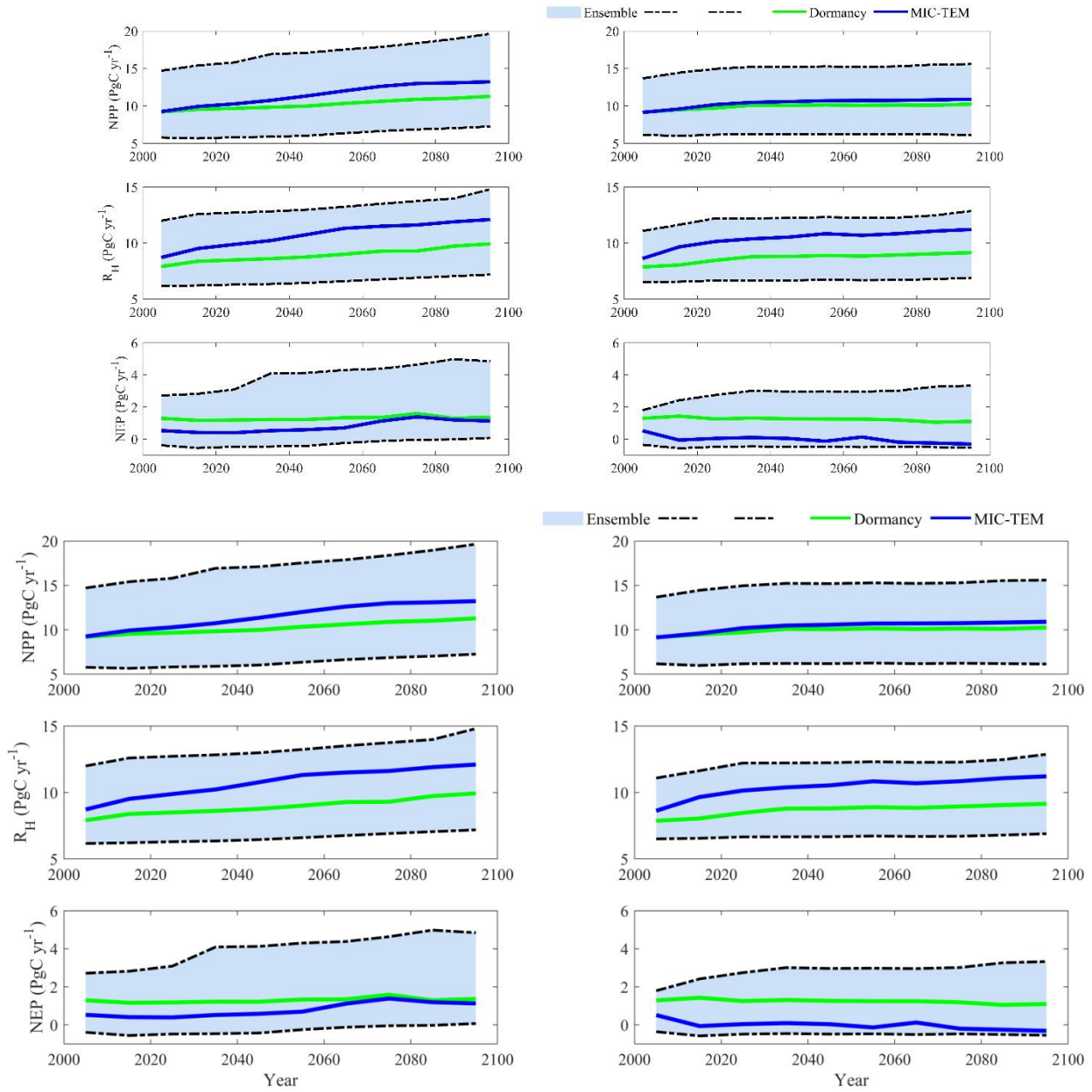
957

958

959

960

961



962

963 Figure 12. Simulated annual net primary production (NPP, top panel), heterotrophic respiration
964 (R_H , center panel) and net ecosystem production (NEP, bottom panel) under RCP 8.5 scenario
965 (left panel) and RCP 2.6 scenario (right panel) by MIC-TEM-dormancy with ensemble of
966 parameters. The decadal running mean is applied. The grey area represents the upper and lower
967 bounds of simulations.

968

969 **Table 1. Parameters associated with detailed microbial dormancy in MIC-TEM-dormancy**
 970

parameter	unit	description	Parameter range	references
m_R	h^{-1}	Specific maintenance rate at active state	[0.001, 0.08]	Wang et al. (2014)
Q_{10mic}	-	Temperature effects on microbial metabolic activity (rate change per 10 °C increase in temperature). Based on 0.65 eV activation energy for soils	[1.5, 3.5]	He et al. (2015)
Q_{10enz}	-	Temperature effects on enzyme activity (rate change per 10 °C increase in temperature). Based on 6% rate increase per degree Celsius	1.79	He et al. (2015)
α	-	the ratio of m_R to the sum of maximum specific growth rate	[0.01, 0.5]	Wang et al. (2014)
β	-	Ratio of dormant microbial maintenance rate to m_R	[0.0005, 0.005]	Wang et al. (2014)
Y_g	-	carbon use efficiency	[0.3, 0.7]	He et al. (2015)
K_s	$mgC\ cm^{-2}$	Half-saturation constant for directly accessible substrate	[0.01, 10]	Wang et al. (2014)
$K_{muptake}$	$mgC\ cm^{-2}$	Half-saturation constant for enzymatic decay of SOC	[200, 1000]	He et al. (2015)
r_{death}	h^{-1}	Potential rate of microbial death	$[2e^{-4}, 2e^{-3}]$	Allison et al. (2010)
$r_{EnzProd}$	h^{-1}	Enzyme production rate of microbe	$[1e^{-4}, 8e^{-4}]$	He et al. (2015)
$r_{enzloss}$	h^{-1}	Enzyme loss rate	[0.0005, 0.002]	Allison et al. (2010)
V_{max}	$mgC\ cm^{-2}\ h^{-1}$	Maximum SOC decay rate	$[1e^{-4}, 5e^{-3}]$	He et al. (2015)

971
 972
 973

974 **Table 2. Site description and measured NEP data used to calibrate MIC-TEM-dormancy**

Site Name	Location (Longitude (degrees) /Latitude (degrees))	Elevation (m)	Vegetation type	Description	Data range	Citations
Univ. of Mich. Biological Station	84.71W 45.56 N	234	Temperate deciduous forest	Located within a protected forest owned by the University of Michigan. Mean annual temperature is 5.83° C with mean annual precipitation of 803mm	01/2005- 12/2006	Gough et al. (2013)
Howland Forest (main tower)	68.74W 45.20N	60	Temperate coniferous forest	Closed coniferous forest, minimal disturbance.	01/2004- 12/2004	Davidson et al. (2006)
UCI-1964 burn site	98.38W 55.91N	260	Boreal forest	Located in a continental boreal forest, dominated by black spruce trees, within the BOREAS northern study area in central Manitoba, Canada.	01/2004- 10/2005	Goulden et al. (2006)
KUOM Turfgrass Field	93.19W 45.0N	301	Grassland	A low-maintenance lawn consisting of cool-season turfgrasses.	01/2006- 12/2008	Hiller et al. (2011)
Atqasuk	157.41W 70.47N	15	Wet tundra	100 km south of Barrow, Alaska. Variety of moist-wet coastal sedge tundra, and moist-tussock tundra surfaces in the more well-drained upland.	01/2005- 12/2006	Oechel et al. (2014);
Ivotuk	155.75W 68.49N	568	Alpine tundra	300 km south of Barrow and is located at the foothill of the Brooks Range and is classified as tussock sedge, dwarf-shrub, moss tundra.	01/2004- 12/2004	McEwing et al. (2015)

975
976
977
978

979 **Table 3. Site description and measured NEP data used to validate MIC-TEM-dormancy**
 980

Site Name	Location (Longitude (degrees) /Latitude (degrees))	Elevation (m)	Vegetation type	Description	Data range	Citations
Bartlett Experimental Forest	71.29W/ 44.06N	272	Temperate deciduous forest	Located within the White Mountains National Forest in north-central New Hampshire, USA, with mean annual temperature of 5.61 °C and mean annual precipitation of 1246mm.	01/2005- 12/2006	Jenkins et al. (2007); Richardson et al. (2007);
Howland Forest (main tower)	68.74W/ 45.20N	60	Temperate coniferous forest	Closed coniferous forest, minimal disturbance.	01/2003- 12/2003	Davidson et al. (2006)
UCI-1964 burn site	98.38W/ 55.91N	260	Boreal forest	Located in a continental boreal forest, dominated by black spruce trees, within the BOREAS northern study area in central Manitoba, Canada.	01/2002- 12/2003	Goulden et al. (2006)
Brookings	96.84W/ 44.35N	510	Grassland	Located in a private pasture, belonging to the Northern Great Plains Rangelands, the grassland is representative of many in the north central United States, with seasonal winter conditions and a wet growing season.	01/2005- 12/2006	Gilmanov et al. (2005)
Atqasuk	157.41W/ 70.47N	15	Wet tundra	100 km south of Barrow, Alaska. Variety of moist-wet coastal sedge tundra, and moist-tussock tundra surfaces in the more well-drained upland.	01/2003- 12/2004	Oechel et al. (2014);
Ivotuk	155.75W/ 68.49N	568	Alpine tundra	300 km south of Barrow and is located at the foothill of the Brooks Range and is classified as tussock sedge, dwarf-shrub, moss tundra.	01/2005- 12/2005	McEwing et al. (2015)

981

982 **Table 4. Site description and measured R_H data used to validate MIC-TEM-dormancy model**

983
984
985
986
987
988
989
990
991
992
993
994

Site	Location (Longitude (degrees) /Latitude (degrees))	Elevation (m)	Vegetation type	Data range	Citations
US-EML	149.25W/ 63.88N	700	Alpine tundra	01/2009- 12/2013	Belshe et al. (2012)
CA-SJ2	104.65W/ 53.95N	580	Boreal forest	01/2004- 12/2008	Coursolle et al. (2006)
US-Ho2	68.75W/ 45.21N	91	Temperate coniferous forest	01/2000- 12/2004	Davidson et al. (2006)
US-UMB	84.71W/ 45.56N	234	Temperate deciduous forest	01/2005- 12/2006	Gough et al. (2013)
US-Ro4	93.07W/ 44.68N	274	Grasslands	01/2016- 12/2017	Griffis et al. (2011)
RU-Che	161.34E/ 68.61N	6	Wet tundra	01/2002- 12/2005	Merbold et al. (2009)

995 **Table 5. Model validation statistics for Dormancy model and MIC-TEM at six sites with NEP data**
 996

997

998	Site Name	Vegetation type	Models	Intercept	Slope	R-square	Adjusted R-square	p-value
999	Ivotuk	Alpine tundra	MIC-TEM	0.85	0.83	0.70	0.67	<0.001
1000			Dormancy	-0.51	1.09	0.75	0.73	<0.001
1001	UCI-1964 burn site	Boreal forest	MIC-TEM	0.18	1.03	0.912	0.9080	<0.001
1002			Dormancy	-0.21	0.96	0.90	0.894	<0.001
1003	Howland Forest (main tower)	Temperate coniferous forest	MIC-TEM	7.29	0.72	0.85	0.83	<0.001
1004			Dormancy	0.27	1.05	0.89	0.88	<0.001
1005	Bartlett Experimental Forest	Temperate deciduous forest	MIC-TEM	-6.05	0.91	0.944	0.941	<0.001
1006			Dormancy	-2.34	1.13	0.93	0.924	<0.001
1007	Brookings	Grassland	MIC-TEM	3.05	0.71	0.84	0.83	<0.001
1008			Dormancy	0.17	0.95	0.90	0.898	<0.001
1009	Atqasuk	Wet tundra	MIC-TEM	7.22	1.85	0.71	0.70	<0.001
1010			Dormancy	0.19	0.82	0.67	0.66	<0.001
1011								

1012 **Table 6. Model validation statistics for Dormancy model and MIC-TEM at six sites with R_H data**
 1013

Site ID	Vegetation type	Models	Intercept	Slope	R-square	Adjusted R-square	RMSE	p-value
US-EML	Alpine tundra	MIC-TEM	2.90	0.91	0.79	0.78	3.55	<0.001
		Dormancy	1.81	0.74	0.87	0.85	2.69	<0.001
CA-SJ2	Boreal forest	MIC-TEM	7.59	1.12	0.84	0.83	9.8	<0.001
		Dormancy	2.6	0.74	0.86	0.85	3.97	<0.001
US-Ho2	Temperate coniferous forest	MIC-TEM	4.07	0.89	0.86	0.84	12.39	<0.001
		Dormancy	6.59	0.71	0.91	0.89	11.83	<0.001
US-UMB	Temperate deciduous forest	MIC-TEM	-4.73	1.32	0.81	0.8	20.05	<0.001
		Dormancy	13.6	0.67	0.85	0.84	12.94	<0.001
US-Ro4	Grassland	MIC-TEM	9.34	0.87	0.81	0.79	11.25	<0.001
		Dormancy	4.81	0.65	0.86	0.84	9.21	<0.001
RU-Che	Wet tundra	MIC-TEM	2.5	0.67	0.72	0.71	6.24	<0.001
		Dormancy	1.96	0.77	0.81	0.79	5.95	<0.001